ACS Catalysis

Research Article

pubs.acs.org/acscatalysis

Generation of HO• Radical from Hydrogen Peroxide Catalyzed by Aqua Complexes of the Group III Metals $[M(H_2O)_n]^{3+}$ (M = Ga, In, Sc, Y, or La): A Theoretical Study

Alexander S. Novikov,[†,‡] Maxim L. Kuznetsov,*[,†,§] Armando J. L. Pombeiro,[†] Nadezhda A. Bokach,[§] and Georgiy B. Shul'pin[⊥]

[†]Centro de Química Estrutural, Complexo I, Instituto Superior Técnico, Technical University of Lisbon, Av. Rovisco Pais, 1049-001 Lisbon, Portugal

[‡]Department of Chemistry, Moscow State Pedagogical University, 3 Nesvizhskiy per., 119021 Moscow, Russian Federation

[§]Department of Chemistry, Saint Petersburg State University, Universitetsky Pr., 26, 198504 Stary Petergof, Russian Federation

[⊥]Semenov Institute of Chemical Physics, Russian Academy of Science, Ulitsa Kosygina, dom 4, 119991 Moscow, Russian Federation

Supporting Information

ABSTRACT: The mechanism of the rate-limiting stage of alkanes oxidation with hydrogen peroxide, that is, formation of the hydroxyl radicals, catalyzed by aqua complexes, $[M(H_2O)_n]^{3+}$ (**1**), of the group III metals exhibiting a unique stable non-zero oxidation state (M = Ga, In, Sc, Y, or La) was theoretically studied in detail at the DFT level. The mechanism involves the substitution of a H_2O ligand for H_2O_2, protolysis of the coordinated H_2O_2, substitution of another H_2O ligand for H_2O_2, generation of the hydroxyl radical upon the homolytic O−O bond cleavage in the key complex $[M(H_2O)_{(n-2)}(H_2O_2)(OOH)]^{2+}$, and closure of the catalytic cycle. The substitution steps proceed via the dissociative mechanism D (M = Ga and Y) or the associative mechanisms A [M = Sc, La, or In (second substitution)] or I_a [M = In (first substitution)]. The general catalytic activity of **1** is determined by three main factors, that is, (i) lability of the complexes, (ii) acidity of the metal-bound ligands, and (iii) the H_2O_2 activation toward the homolytic O−O bond cleavage. The H_2O_2 activation, in turn, depends on the strength of the M−O_2H_2 bond, delocalization of the spin density within a coligand (OOH^-), and ability of the coligand to be easily oxidized. The calculations predict that the catalytic activity of **1** increases along the row of the metals Al ≈ La < Y ≈ In < Sc < Ga.

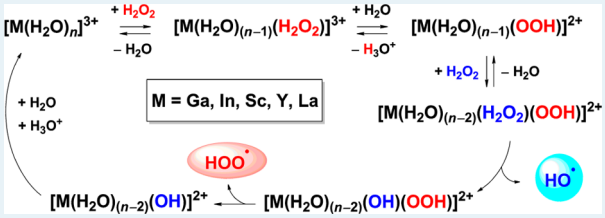

KEYWORDS: *alkanes, DFT calculations, gallium, homogeneous catalysis, hydrogen peroxide, hydroxyl radical, indium, lanthanum, oxidation, reaction mechanism, water exchange, yttrium*

INTRODUCTION

Hydrocarbons, in general, and alkanes, in particular, are the most abundant and cheapest carbon raw material, and their functionalization leading to industrially valuable products (alcohols, esters, aldehydes, ketones, carboxylic acids, amines, etc.) attracts much current attention.[1] One of the most important types of alkane functionalization is their oxidation to the corresponding alcohols or ketones. The high chemical inertness of alkanes toward oxidation requires the application of catalysts for these processes. Transition metal complexes or metal oxides are usually used as such catalysts while various peroxo compounds (hydrogen peroxide (H_2O_2), organic peroxides (ROOH), peroxomono or disulfate ($KHSO_5$, $K_2S_2O_8$)) as well as some transition metal complexes or oxides with the metal in a high oxidation state (e.g., MnO_4^-, OsO_4, or RuO_4)[2] are typically applied as oxidants in these reactions. Among the oxidants, hydrogen peroxide is the most attractive from the ecological ("green reagent") and economical points of view, water being the only product of the H_2O_2 reduction and O_2 being the only byproduct.

Two main types of mechanisms are usually considered for the oxidation of alkanes with H_2O_2, that is, nonradical and radical mechanisms. The first one was proposed by Bray and Gorin for the oxidation of alkanes with the Fenton reagent (Fe^{II} + H_2O_2) in one of a few possible routes,[3] and it involves the ferryl ion Fe^{IV}=O^{2+} as an oxidant of alkanes. The second one includes the generation of highly reactive HO• radicals, which then abstract a hydrogen atom from the alkane molecule R−H giving corresponding alkyl radical R•. The latter species reacts with molecular oxygen affording the alkylperoxo radical ROO• (Scheme 1), which, in turn, is transformed into the final product(s) via a multistep radical process.[4] The rate-limiting step of this reaction is the generation of the hydroxyl radicals.

The first mechanistic proposal for the formation of HO• radicals from H_2O_2 in the presence of the Fe(II) aqua complex was formulated by Haber and Weiss.[5] This mechanism involves

Received: February 26, 2013
Revised: April 15, 2013
Published: April 22, 2013

Scheme 1. Radical Mechanism of the Alkanes Oxidation with H_2O_2[a]

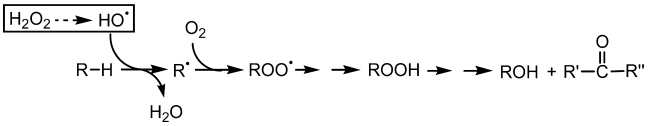

[a]The rate-limiting step of the whole process is boxed.

the one-electron oxidation of Fe(II) to Fe(III) accompanied by the homolytic O−O bond cleavage in the H_2O_2 molecule (reaction 1). The initial complex of Fe(II) may then be restored by reduction of the Fe(III) species with H_2O_2 (reaction 2). This proposal was revised later in a number of works.[6,7] In a modified mechanism[6] (Scheme 2), two H_2O_2

Scheme 2. Mechanism of the Iron-Catalyzed HO• Radical Generation Involving Two H_2O_2 Molecules

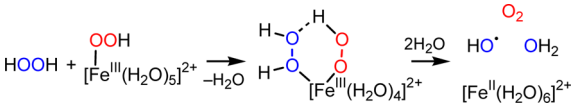

molecules are involved in the process. The first one is responsible for the formation of the HOO^- ion, which is ligated to the iron center. The second H_2O_2 molecule being also coordinated to the Fe cation undergoes the homolytic O−O bond cleavage.

$$[Fe^{II}(H_2O)_6]^{2+} + H_2O_2 \rightarrow [Fe^{III}(H_2O)_5(OH)]^{2+} + HO^{\bullet} + H_2O \quad (1)$$

$$[Fe^{III}(H_2O)_5(OH)]^{2+} + H_2O_2 \rightarrow [Fe^{II}(H_2O)_6]^{2+} + HOO^{\bullet} \quad (2)$$

Even today it is still unclear which mechanism (radical or nonradical) is operating (or predominant) when alkanes are oxidized with the Fenton reagent ($Fe^{II} + H_2O_2$).[7] Meanwhile, in the case of many catalytic systems based on other transition metals, the radical pathway seems to be preferable.[1b] When the metal of a catalyst is in its highest oxidation state, a modified mechanism of the HO• generation was proposed[4] and then theoretically studied[8] for metals such as V(V) and Re(VII). It includes the initial reduction of the metal upon elimination of the HOO• radicals from the metal-bound H_2O_2, while the HO• radical appears at a latter stage (Scheme 3).

Scheme 3. Simplified Mechanism of the HO• Radical Generation Catalyzed by Transition Metal Complexes with the Metal in the Highest Oxidation State[a]

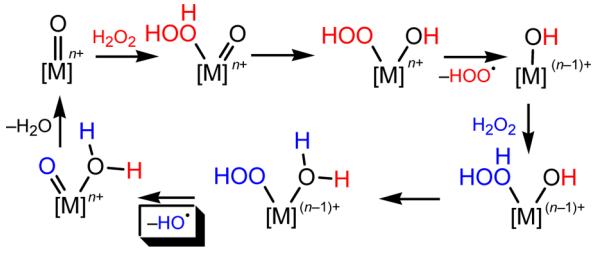

[a]The metal oxidation state is indicated.

In contrast to transition metals of groups IV−VIII, the oxidation of alkanes by peroxides in the presence of metals of groups II and III is rather rare. Examples include mostly heterogeneous reactions in which species such as aluminum oxide, aluminosilicates, aluminophosphates,[9] or magnesium oxide[10] are used as a support or serve as catalysts themselves.[11] Additionally, magnesium powder, various simple Ca salts, and lanthanide-containing compounds were applied as catalysts for the reaction of carboxylation of alkanes with carbon monoxide and $K_2S_2O_8$ as oxidant in trifluoroacetic acid medium.[12]

Recently, it was found[13] that the simple aluminum aqua complex $[Al(H_2O)_6]^{3+}$ [introduced into the reaction mixture in the form of $Al(NO_3)_3$] efficiently catalyzes the homogeneous oxidation of alkanes with H_2O_2 in aqueous CH_3CN. The experimental kinetic data and the reaction selectivity parameters indicate that the reaction occurs via a radical mechanism with participation of the HO• radical. At the same time, the mechanism of the HO• generation in this Al-containing system should be of a fundamentally new type. Indeed, all radical pathways discussed above require the change of the metal oxidation state, which is necessary for the formation of active oxidizing species. However, Al, as well as other metals of group II (Be, Mg, Ca, Sr, Ba, Zn, and Cd) and group III (Ga, In, Sc, Y, and some Ln), has only one stable nonzero oxidation state.

The mechanism of the HO• generation in the $[Al(H_2O)_6]^{3+}/H_2O_2$ system remained a mystery until recently. In our previous work,[14] we proposed for the first time and theoretically calculated such a mechanism. It includes the substitution of one of the water ligands in $[Al(H_2O)_6]^{3+}$ for the hydrogen peroxide molecule, protolysis of the coordinated H_2O_2, substitution of a second H_2O for H_2O_2, and the homolytic HO−OH bond cleavage to give HO• radicals (see Scheme 4 generalized for

Scheme 4. Mechanism of the HO• Radical Generation with the Systems $[M(H_2O)_n]^{3+}/H_2O_2/CH_3CN-H_2O$ (M = Al, Ga, In, Sc, Y, or La)

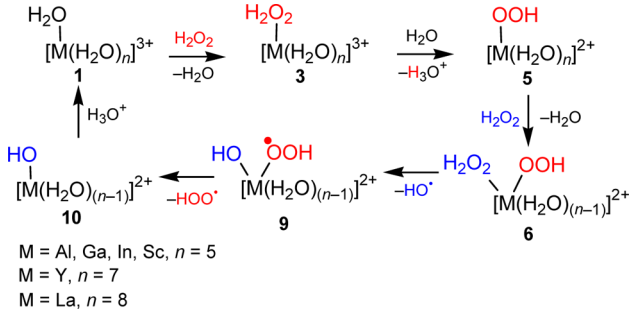

other metals of group III). The subsequent elimination of the HOO• radical, saturation of the coordination sphere by a water molecule, and protonation of the derived hydroxo complex complete the catalytic cycle. Within this mechanism, the great activation of the H_2O_2 molecule in complex $[Al(H_2O)_4(H_2O_2)(OOH)]^{2+}$ toward the homolytic O−O bond cleavage provides the relatively easy formation of the HO• radicals ($\Delta G_s^{\ddagger}$ value of 25.6 kcal/mol) without any change of the metal oxidation state.

In this work, we extend to other metals of group III the theoretical investigation of the HO• radical formation from H_2O_2 catalyzed by simple aqua complexes. The essential goal of this study is to obtain information about the possibility of HO• generation in the systems $[M(H_2O)_n]^{3+}/H_2O_2/CH_3CN-H_2O$ (M = Ga, In, Sc, Y, or La) and, hence, about perspectives of the application of these metals and their compounds for the

dx.doi.org/10.1021/cs400155q | ACS Catal. 2013, 3, 1195−1208

homogeneous oxidation of alkanes. Details of the plausible mechanism of the HO• generation are discussed and main factors determining the catalytic activity of the aqua complexes are analyzed.

COMPUTATIONAL DETAILS

The full geometry optimization of all structures and transition states (TS) has been carried out at the DFT/HF hybrid level of theory using Becke's three-parameter hybrid exchange functional in combination with the gradient-corrected correlation functional of Lee, Yang, and Parr (B3LYP)[15] with the help of the Gaussian-03[16] program package. The standard basis set 6-311+G(d,p)[17] was applied for all atoms, in the case of complexes of Al, Ga, and Sc, and for nonmetal atoms, in the case of complexes of In, Y, and La. The quasi-relativistic Stuttgart pseudopotentials describing 46 (In and La) or 28 (Y) core electrons and the appropriate contracted basis sets (4s4p)/[2s2p] (In),[18a] (7s6p5d)/[5s4p3d] (La),[18b] or (8s7p6d)/[6s5p3d] (Y)[19] were employed for In, Y, and La. These basis sets were augmented by addition of two d-functions (exponents (exp) 0.231 and 0.069) and two f-functions (exp 0.4487 and 0.1)[20] for the In atoms and one f-function (exp 1.0)[21] for the Y and La atoms. No symmetry operations have been applied for any of the structures calculated.

Taking into account the importance of the consideration of the second coordination sphere in the calculations of solvent effects for reactions involving highly charged species, one solvent molecule (H_2O or H_2O_2) was included explicitly in the second shell of the calculated structures except intermediates and transition state of the associative mechanism of the water substitutions (consult Tables S2−S5 in Supporting Information for each particular case). In the latter cases, the external solvent molecule was not added to preserve the number of molecules participating in the reaction and, hence, to minimize the error of the entropy estimates. For simplicity, the second-sphere solvent molecules are not shown in the formulas of complexes in the text and schemes.

As indicated in the previous[14] and this work (as discussed later), the combination of the B3LYP functional, the basis sets used, and the model with one explicit solvent molecule in the second coordination sphere provide excellent agreement between the calculated and experimental activation energies of the water substitution reactions, two principal steps of the calculated mechanism. Additionally, the O−O bond dissociation energy in H_2O_2 calculated at this level of theory (48.7 kcal/mol, the total gas-phase energy scale) is very close to the experimental value of 48.75 ± 0.005 kcal/mol.[22]

Restricted approximations for the structures with closed electron shells and unrestricted methods for the structures with open electron shells have been employed. For several structures, instability of wave functions was found. In these cases, the following reoptimization of the wave functions was carried out to achieve a stable solution using the keyword STABLE(Opt) in Gaussian-03.

The Hessian matrix was calculated analytically for the optimized structures in order to prove the location of correct minima (no imaginary frequencies) or saddle points (only one imaginary frequency), and to estimate the thermodynamic parameters, the latter being calculated at 25 °C. The nature of all transition states was investigated by the analysis of vectors associated with the imaginary frequency and by the calculations of the intrinsic reaction coordinates (IRC) using the Gonzalez−Schlegel method.[23]

Total energies corrected for solvent effects (E_s) were estimated at the single-point calculations on the basis of gas-phase geometries using the polarizable continuum model in the CPCM version[24] with CH_3CN or, in some cases, H_2O as solvents. The entropic term for the CH_3CN solvent (S_s) was calculated according to the procedure described by Wertz[25] and Cooper and Ziegler[26] using eqs C1−C4

$$\Delta S_1 = R \ln V^s_{m,liq}/V_{m,gas} \quad \text{(C1)}$$

$$\Delta S_2 = R \ln V^\circ_m/V^s_{m,liq} \quad \text{(C2)}$$

$$\alpha = \frac{S^{\circ,s}_{liq} - (S^{\circ,s}_{gas} + R \ln V^s_{m,liq}/V_{m,gas})}{(S^{\circ,s}_{gas} + R \ln V^s_{m,liq}/V_{m,gas})} \quad \text{(C3)}$$

$$\begin{aligned} S_s &= S_g + \Delta S_{sol} \\ &= S_g + [\Delta S_1 + \alpha(S_g + \Delta S_1) + \Delta S_2] \\ &= S_g + [(-12.21 \text{ cal/(mol·K)}) - 0.23 \\ &\quad (S_g - 12.21 \text{ cal/(mol·K)}) + 5.87 \text{ cal/(mol·K)}] \end{aligned} \quad \text{(C4)}$$

where S_g = gas-phase entropy of solute, ΔS_{sol} = solvation entropy, $S^{\circ,s}_{liq}$, $S^{\circ,s}_{gas}$, and $V^s_{m,liq}$ = standard entropies and molar volume of the solvent in liquid or gas phases (149.62 and 245.48 J/(mol·K) and 52.16 mL/mol, respectively, for CH_3CN), $V_{m,gas}$ = molar volume of the ideal gas at 25 °C (24 450 mL/mol), and V°_m = molar volume of the solution corresponding to the standard conditions (1000 mL/mol). The S_s values for the H_2O solvent were calculated using eq C5.[26]

$$\begin{aligned} S_s = S_g &+ [(-14.3 \text{ cal/(mol·K)}) - 0.46(S_g - 14.3 \text{ cal/(mol·K)}) \\ &+ 7.98 \text{ cal/(mol·K)}] \end{aligned} \quad \text{(C5)}$$

The enthalpies and Gibbs free energies in solution (H_s and G_s) were estimated using the expressions $H_s = E_s + H_g - E_g$ and $G_s = H_s - TS_s$, where E_g and H_g are the gas-phase total energy and enthalpy. The relative energies discussed in the text are Gibbs free energies in solution if not stated otherwise.

In the experimental study of the oxidation of alkanes with the system $[Al(H_2O)_6]^{3+}/H_2O_2$, the mixed solvent CH_3CN−H_2O was used. The water part of this solvent was approximated by the explicit inclusion of one H_2O molecule in the second coordination shell whereas the acetonitrile part of the solvent was approximated by the CPCM calculations of the bulky solvent effect for CH_3CN.

The Wiberg bond indices (B_i)[27] were computed for the concerted water substitution reactions by using the natural bond orbital (NBO) partitioning scheme.[28] The reaction synchronicity (S_y) was calculated using the formula[29]

$$S_y = 1 - (2n - 2)^{-1} \sum_{i=1}^{n} \frac{|\delta B_i - \delta B_{av}|}{\delta B_{av}} \quad \text{(C6)}$$

where n is the number of bonds directly involved in the reaction (e.g., $n = 2$ for the concerted water substitution reactions). The S_y value varies from 0 (for stepwise mechanism) to 1 (for perfectly synchronous reactions). δB_i is the relative variation of a given B_i at the transition state relative to reactants (R) and products (P), and it is calculated as

$$\delta B_i = \frac{B_i^{TS} - B_i^R}{B_i^P - B_i^R} \quad \text{(C7)}$$

The average value of δB_i (δB_{av}) is defined as

$$\delta B_{av} = n^{-1} \sum_{i=1}^{n} \delta B_i \quad \text{(C8)}$$

This value may be used as a measure of the advancement of TS along the reaction path. If $\delta B_{av} < 0.5$, TS is "early"; if $\delta B_{av} > 0.5$, TS is "late".

RESULTS AND DISCUSSION

1. Starting Aqua Complexes. Aqua complexes $[M(H_2O)_n]^{3+}$ are starting catalytic species, which initiate a cycle for the generation of the HO• and HOO• radicals. In accord with the experimental data, the aqua complexes of Ga^{3+} and In^{3+} exist in solution as hexahydrates $[M(H_2O)_6]^{3+}$ with octahedral geometry.[30] The predominant form of the scandium aqua complex in diluted solutions is also $[Sc(H_2O)_6]^{3+}$,[31] although for more concentrated or strongly acidic solutions, the formation of the heptahydrate and even octahydrate was

dx.doi.org/10.1021/cs400155q | ACS Catal. 2013, 3, 1195−1208

observed.[32] The most stable aqua complexes of Y^{3+} and La^{3+} in both solid state and solution are octa- and enneahydrates, respectively.[33] The coordination polyhedron of $[Y(H_2O)_8]^{3+}$ is square antiprism (Figure 1, i), which is symmetric in solution[33a] but distorted in the solid state.[33c,d] The polyhedron of $[La(H_2O)_9]^{3+}$ is tricapped trigonal prism (Figure 1, ii).[33e]

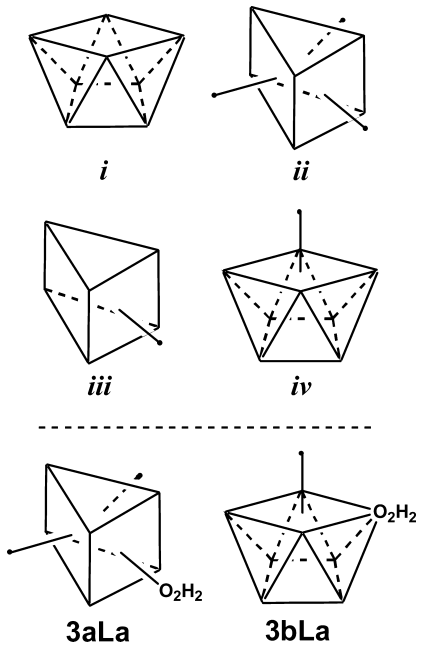

Figure 1. Coordination polyhedra realized for **1Y**, **2La**, and **3Y** (i), **1La** (ii), **2Y** (iii), and **3La** (ii and iv). Water ligands and metal atoms are not shown.

The calculated structures of $[M(H_2O)_6]^{3+}$ [M = Ga, (**1Ga**), In (**1In**), and Sc (**1Sc**)], $[Y(H_2O)_8]^{3+}$ (**1Y**), and $[La(H_2O)_9]^{3+}$ (**1La**) reasonably reproduce the experimental polyhedra and bond lengths. The calculated mean M−O bond lengths deviate from the corresponding experimental EXAFS, XANES, and LAXS solution data[32a,33a,b,34] by 0.05 Å (**1Ga**, **1La**), 0.02 Å (**1In**, **1Sc**), and 0.07 Å (**1Y**).

2. Formation of the First Hydrogen Peroxide Complex. For all discussed aqua complexes, the water exchange processes are known to occur in solution.[35] In the presence of a significant amount of H_2O_2, which has donor properties close to H_2O, it is very expected that the similar substitution of one water ligand for a hydrogen peroxide molecule is also realized. For the ligand substitution reactions, two global mechanisms are recognized, that is, concerted (interchange, type I, via one transition state) and stepwise (via an intermediate). The stepwise mechanism may be dissociative or associative (D or A, according to the classification of Langford and Gray[36]).

i. Dissociative Mechanism. A mechanism of this type was found for aqua complexes of all metals under study (Scheme 5, D). It includes the elimination of one water ligand to the second coordination sphere via transition states **TS1** to give an intermediate with reduced coordination number $[M(H_2O)_5]^{3+}$ (M = Ga (**2Ga**), In (**2In**), and Sc (**2Sc**)), $[Y(H_2O)_7]^{3+}$ (**2Y**), and $[La(H_2O)_8]^{3+}$ (**2La**). The coordination polyhedron of intermediates **2Ga**, **2In**, and **2Sc** is trigonal bipyramid, whereas those for **2Y** and **2La** are capped trigonal prism iii and square antiprism i, respectively (Figure 1). Then, at the next step, a

Scheme 5. Dissociative (D), Associative (A) and Interchange (I_a) Mechanisms of the Water Substitution for Hydrogen Peroxide in Aqua Complexes 1[a]

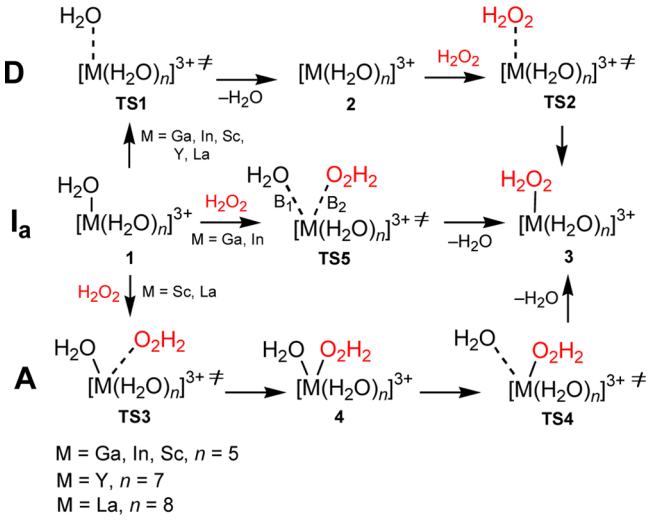

[a]Wiberg bond indices B_1 and B_2 for the breaking and forming bonds are indicated for **TS5**.

H_2O_2 molecule coordinates to the metal, and complexes $[M(H_2O)_5(H_2O_2)]^{3+}$ (M = Ga (**3Ga**), In (**3In**), and Sc (**3Sc**)), $[Y(H_2O)_7(H_2O_2)]^{3+}$ (**3Y**), and $[La(H_2O)_8(H_2O_2)]^{3+}$ (**3La**) are formed via **TS2**. The coordination polyhedra of **3Ga**−**Y** are octahedron or square antiprism i, while for **3La** one isomer was found for each tricapped trigonal prism ii (**3aLa**) and capped square antiprism iv (**3bLa**) polyhedron (Figure 1), **3aLa** being slightly more stable. The M−O_2H_2 bond in **3** is significantly longer (by 0.07−0.39 Å) compared with the M−OH_2 bonds indicating a weaker binding between the metal and hydrogen peroxide (see Table S1 in Supporting Information for the bond lengths and bond energies).

The energies of corresponding **TS1** and **TS2** are rather similar with the difference of 0.2−2.2 kcal/mol. The rate-limiting step of this substitution reaction is the first one for Ga, In, and La, and it is the second one for Sc and Y.

ii. Associative Mechanism. The mechanism of this type was found only for Sc and La (Scheme 5, A). In the case of Sc, it involves the formation of the hepta-coordinated intermediate $[Sc(H_2O)_6(H_2O_2)]^{3+}$ (**4Sc**) upon addition of one H_2O_2 molecule to the first coordination sphere via **TS3Sc**. For the intermediate **4Sc**, several isomers of the distorted capped trigonal prismatic or pentagonal bipyramidal structures were found, and isomer **4aSc** is the most stable one (Figure 2, Tables S3 and S4, Supporting Information). The energy of the hepta-coordinated species **4aSc** is only 0.8 kcal/mol higher than that of the hexahydrate $[Sc(H_2O)_6](H_2O_2)^{3+}$ **1Sc**. This is consistent with the experimental observations of both hexa- and heptahydrates of scandium in solution depending on concentration and counterion.[31,32a]

At the next step, the elimination of a water ligand in **4aSc** leads to the substitution product $[Sc(H_2O)_5(H_2O_2)]^{3+}$ (**3Sc**, Scheme 5). Taking into account that there are several nonequivalent water molecules in **4aSc** (Figure 2), two different transition states were found for this step (**TS4aaSc** and **TS4abSc**) with **TS4aaSc** as the most stable one. The second step of the substitution is the rate-limiting one.

dx.doi.org/10.1021/cs400155q | *ACS Catal.* 2013, 3, 1195−1208

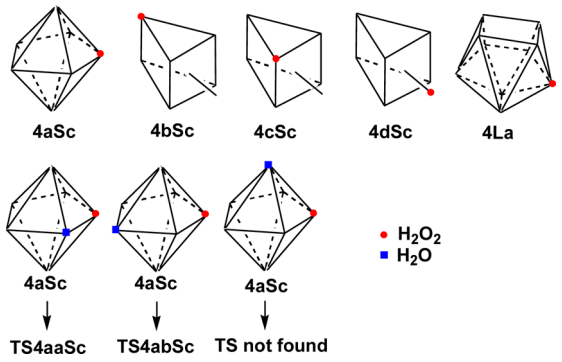

Figure 2. Coordination polyhedra of **4Sc** and **4La** and nonequivalent water ligands in **4aSc**. In the last three polyhedra, the nonequivalent H_2O molecules eliminating upon the formation of **TS4aSc** are shown. Other water ligands and metal atoms are omitted.

In the case of La, the deca-coordinated intermediate $[La(H_2O)_9(H_2O_2)]^{3+}$, **4La** (Figure 2), and transition states **TS3La** and **TS4La** corresponding to its formation from **1La** and decomposition to **3La** were located. Both **TS3La** and **TS4La** lie very close to **4La** on the reaction path. However, the analysis of the potential energy surface (PES) unambiguously confirms the nature of these TSs (see Supporting Information). The energies of **TS3La** and **TS4La** are similar (5.3 and 4.8 kcal/mol relative to **1La**). In fact, the character of the PES indicates that, in the case of La, this mechanism may be described as a borderline case between stepwise type A and concerted type I_a.

No intermediates **4** of the associative mechanism were found for Ga, In, and Y. All attempts at their location resulted in the extrusion of H_2O or H_2O_2 molecule from the first coordination sphere.

iii. Concerted (Interchange) Mechanism. This mechanism was found for Ga and In, and it involves the formation of one transition state, **TS5Ga** or **TS5In**, that directly connects the initial complex **1** and the substitution product **3** (Scheme 5, I_a). The principal feature of **TS5In** is the same In−O_2H_2 bond length as in the product **3In** (2.197 Å), while the breaking In−OH_2 bond is clearly elongated to 2.636 Å. That is, this transition state is close to the product on the reaction path.

Previously,[37] we proposed to use the Wiberg bond indices for the analysis of the features of concerted substitutions. It was shown that the parameter S_y (eq C6 in Computational Details) serves as a quantitative measure of the reaction synchronicity varying from 0 (stepwise mechanism A or D) to 1 (concerted mechanism I). Comparison of the relative Wiberg bond index variations for the breaking and forming bonds (δB_1 and δB_2, eq C7 in Computational Details) provides an information about the mechanism type (I, I_a, or I_d). The average value of the relative Wiberg bond index variations (δB_{av}, eq C8 in Computational Details) gives information about the advancement of TS along the reaction path.

For the reaction **1In** → **TS5In** → **3In**, the following parameters were obtained: δB_1 = 0.57, δB_2 = 0.99, S_y = 0.73, and δB_{av} = 0.78. These values indicate that the concerted mechanism has clearly associative character (I_a) with the In−O_2H_2 bond formation preceding the In−OH_2 bond cleavage by 27%, and **TS5In** is indeed "late" and has a product-like character.

The transition state **TS5Ga** is more "half-way" on the reaction path, the δB_{av} value being 0.60. At the same time, the mechanism is more asynchronous (S_y = 0.53) but still of the associative I_a type (δB_1 = 0.32 and δB_2 = 0.88).

iv. Activation and Reaction Energies. An inspection of the calculated activation and reaction energies ($\Delta G_s^{\ddagger}$ and ΔG_s) (Table 1, Figure 3) allows us to make the following

Table 1. Calculated Gibbs Free Energies of Activation ($\Delta G_s^{\ddagger}$) and Reaction (ΔG_s) in Solution (in kcal/mol) for the H_2O-for-H_2O_2 Substitution in 1

metal	mechanism type	reaction	$\Delta G_s^{\ddagger}$	ΔG_s
Ga	D	**1Ga** → **2Ga** via **TS1Ga**	13.5	7.3
		2Ga → **3Ga** via **TS2Ga**	4.1	−2.6
	I_a	**1Ga** → **3Ga** via **TS5Ga**	22.2	4.7
In	D	**1In** → **2In** via **TS1In**	17.5	13.4
		2In → **3In** via **TS2In**	3.4	−8.3
	I_a	**1In** → **3In** via **TS5In**	13.7	5.1
Sc	D	**1Sc** → **2Sc** via **TS1Sc**	17.1	12.5
		2Sc → **3Sc** via **TS2Sc**	5.5	−9.0
	A	**1Sc** → **4Sc** via **TS3Sc**	4.3	0.7
		4Sc → **3Sc** via **TS4Sc**	7.5	2.7
Y	D	**1Y** → **2Y** via **TS1Y**	7.6	3.7
		2Y → **3Y** via **TS2Y**	4.1	−1.4
La	D	**1La** → **2La** via **TS1La**	6.2	3.0
		2La → **3La** via **TS2La**	2.2	0.1
	A	**1La** → **4La** via **TS3La**	5.3	4.1
		4La → **3La** via **TS4La**	0.8	−0.9

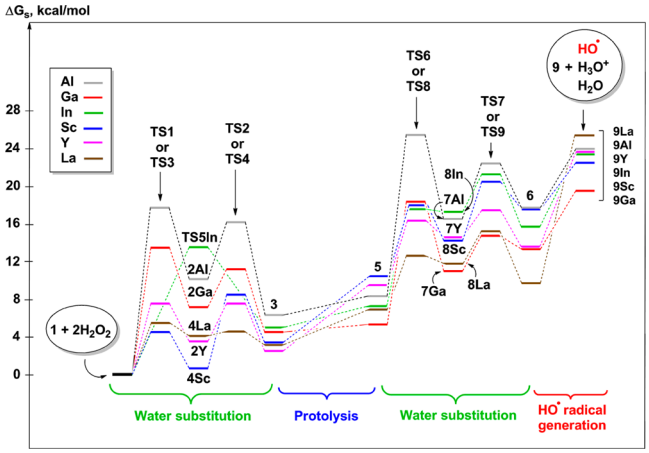

Figure 3. Energy profiles for the most plausible routes of the HO• radical formation catalyzed by aqua complexes of the group III metals (only metal-containing species are indicated except the first and the last levels).

conclusions. First, the most plausible mechanisms of the H_2O-to-H_2O_2 substitution in $[M(H_2O)_n]^{3+}$ are dissociative D for M = Al,[14] Ga, and Y, associative A for M = Sc, and associative interchange I_a for M = In. Other mechanisms that were also found for Ga (I_a), In (D), and Sc (D) are clearly less favorable. In the case of La, the associative mechanism A is only slightly more favorable than the dissociative one D (by 0.9 kcal/mol). Such a situation can be explained by a high lability of the La complexes and by the great variety of stable coordination numbers for this metal.

Second, the overall activation barrier of the substitution decreases along the row of the metals Al > In ≈ Ga > Sc > Y > La varying from 17.9 to 5.3 kcal/mol (Figure 3). Third, the hydrogen peroxide adducts **3** are slightly less thermodynami-

dx.doi.org/10.1021/cs400155q | ACS Catal. 2013, 3, 1195−1208

cally stable relative to the initial aqua complexes for all metals. The complexes of the group IIIA metals (**3Al**, **3Ga**, and **3In**) are less stable than those of the group IIIB metals (**3Sc**, **3Y**, and **3La**), ΔG_s of formation being within 4.7−6.2 and 2.3−3.5 kcal/mol for the first and second group, respectively.

v. Comparison with Experimental Data. To our knowledge, there are no experimental data for the substitution of water for hydrogen peroxide in **1** (although some experimental kinetic data for this reaction were recently published for the Fe(III) species[7k]). However, the similar water exchange reaction for some of these aqua complexes is rather well studied. The results based on kinetic ^{17}O NMR experiments indicate that the water exchange in $[Ga(H_2O)_6]^{3+}$ occurs via a dissociatively activated mechanism.[35c,38] The experimentally determined Gibbs free energy of activation is 13.9 kcal/mol.[35c] The $\Delta G_s^{\ddagger}$ value calculated in this work for the H_2O-for-H_2O_2 substitution is 13.5 kcal/mol. It is important that for the dissociative mechanism the activation barrier does not depend on the nature of incoming ligand and, hence, the kinetic data for water exchange and H_2O-for-H_2O_2 substitution in $[Ga(H_2O)_6]^{3+}$ are directly comparable. Thus, our computational results are in perfect qualitative (mechanism type) and quantitative (activation energy value) agreement with experiment.

The experimental data for the water exchange in $[In(H_2O)_6]^{3+}$ indicate the associatively activated mechanism for this process.[35d,38] The theoretical results obtained previously by Rotzinger, Merbach, and coauthors[39] support the stepwise associative water exchange (type A). However, our calculations reveal that the most plausible mechanism of the H_2O-for-H_2O_2 substitution is associative interchange (type I_a) since no intermediate $[In(H_2O)_6(H_2O_2)]^{3+}$ was found for this process (see above). At the same time, we were able to locate the hepta-coordinated intermediate $[In(H_2O)_7]^{3+}$ of the mechanism type A for water exchange using the same computational model and method as described in the Computational Details section, consistent with experimental[35d,38] and theoretical[39] data. Keeping in mind that the nature of the incoming ligand plays a crucial role for the associative pathways, the successful location of $[In(H_2O)_7]^{3+}$ demonstrates that the difference of the mechanisms for water exchange (A) and for H_2O-for-H_2O_2 substitution (I_a) is not due to computational method or model restrictions, but it has a real physical basis.

The water exchange in $[In(H_2O)_6]^{3+}$ is very fast, and therefore, only a lower limit of the reaction rate and an upper limit of the Gibbs free energy of activation (≤7.9 kcal/mol)[35d,39] were experimentally measured for this process. Our calculations show that the substitution of H_2O for H_2O_2 requires a higher energy ($\Delta G_s^{\ddagger}$ = 13.7 kcal/mol), and this is due to the different mechanisms operating for these processes.

The mechanism of water exchange in aqua complexes of the heaver lanthanides (Ln = Eu−Lu) was experimentally found to be associatively activated.[35a,40] To our knowledge, there are no experimental kinetic data on the water exchange for the La aqua complex. However, the kinetics of formation of the sulfate lanthanide complexes was measured for the whole series except Pm.[41] The corresponding rate constant for La is intermediate between that for Ho and Er. Taking into account that the rate constants for the sulfate formation correlate well with the water exchange rate constants (Figure 4), it can be expected that the rate constant and activation barrier of the water substitution for La are also close to those for the Ho and Er, that is, in the ranges of (1.3−2.1) × 10^8 and 6.1−6.4 kcal/mol[40d,e] (in terms

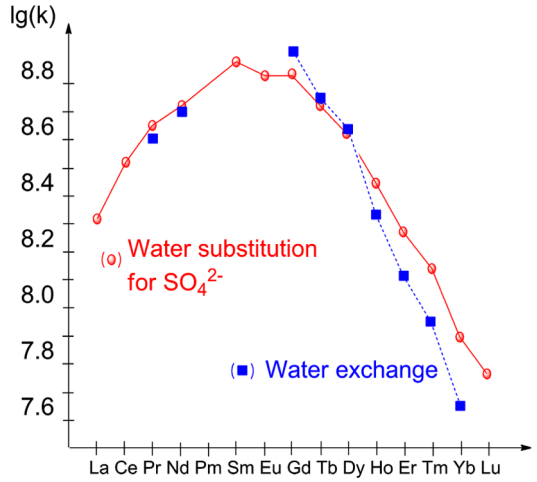

Figure 4. Rate constants of the water exchange and water substitution for SO_4^{2-} in lanthanide aqua complexes.

of Gibbs free energies). The calculated $\Delta G_s^{\ddagger}$ value for the H_2O-for-H_2O_2 substitution in $[La(H_2O)_9]^{3+}$ is 5.3 kcal/mol, which is in good agreement with the thus estimated experimental values.

We were unable to find any experimental data for the water exchange in Sc and Y aqua complexes. At the same time, theoretical calculations[42] predict that in the case of Sc the mechanism should be of associative type A. Our calculations indicate that the same mechanism is operating also for the H_2O-for-H_2O_2 substitution reaction.

3. Protolysis of the Hydrogen Peroxide Complex. Aqua complexes of the group III elements undergo an effective protolysis in aqueous solutions to give the corresponding hydroxo-species. In the case of the hydrogen peroxide adducts **3**, there are two ligands capable of participating in the proton transfer, H_2O and H_2O_2 (Scheme 6). Taking into account the

Scheme 6. Protolysis of Complexes 3

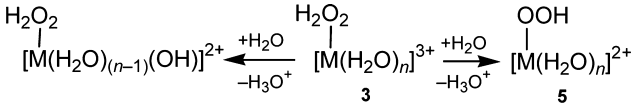

M = Ga, In, Sc, n = 5
M = Y, n = 7
M = La, n = 8

more acidic nature of H_2O_2 compared with H_2O, the protolysis of ligated hydrogen peroxide is more efficient, which was confirmed for $[Al(H_2O)_5(H_2O_2)]^{3+}$ by theoretical calculations.[14] Hence, the protolysis of **3** results in a predominant formation of the hydroperoxo complexes $[M(H_2O)_5(OOH)]^{2+}$ (M = Ga (**5Ga**), In (**5In**), Sc (**5Sc**)), $[Y(H_2O)_7(OOH)]^{2+}$ (**5Y**), and $[La(H_2O)_8(OOH)]^{2+}$ (**5La**).

The CPCM method and the model with one explicit solvent molecule in the second sphere perfectly describe reactions in which the number of species with the same charge is preserved (e.g., ligand substitution, see above). However, this method and model fail if this number is not preserved (e.g., the protolysis of **3** when there is one species with the charge 3+ before the reaction ($[M(H_2O)_n(H_2O_2)]^{3+}$) and there are two species with the charges 2+ and 1+ after the reaction ($[M(H_2O)_n(OOH)]^{2+}$ and H_3O^+). Indeed, the calculated pK_a value of $[Al(H_2O)_6]^{3+}$

dx.doi.org/10.1021/cs400155q | ACS Catal. 2013, 3, 1195−1208

with one explicit water molecule in the second sphere is −3.8,[14] while the experimental value is ca. 5.[43]

Therefore, in order to estimate the ΔG_s values of protolysis of **3**, we used experimental pK_a values of the corresponding aqua complexes **1**[44] and the thermodynamic cycle (Figure 5).

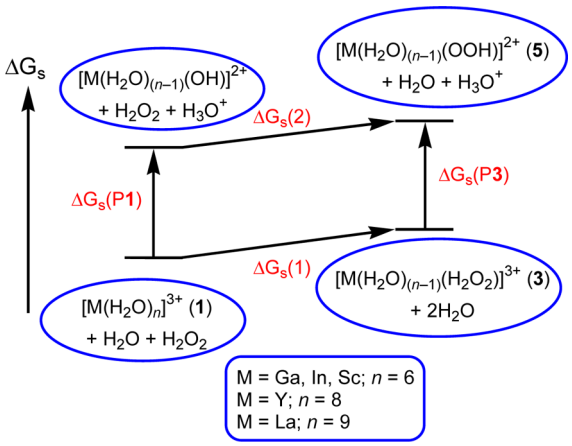

Figure 5. Thermodynamic cycle for the calculations of ΔG_s values of protolysis of **3** [ΔG_s(P3)] using the experimental value ΔG_s(P1) and calculated values $\Delta G_s(1)$ and $\Delta G_s(2)$.

The ΔG_s values of protolysis of **1** in water solution [ΔG_s(P1)] were estimated from the experimental pK_a values using the equation pK_a = $\Delta G_s/(2.303RT)$ − 1.74.[45] The ΔG_s values of the processes

$$[M(H_2O)_n]^{3+} + H_2O_2 \rightarrow [M(H_2O)_{(n-1)}(H_2O_2)]^{3+} + H_2O \qquad \Delta G_s(1)$$

and

$$[M(H_2O)_{(n-1)}(OH)]^{2+} + H_2O_2 \rightarrow [M(H_2O)_{(n-1)}(OOH)]^{2+} + H_2O \qquad \Delta G_s(2)$$

(n = 6 for M = Ga, In, or Sc; n = 8 for M = Y; n = 9 for M = La) in water solution involved in the thermodynamic cycle were calculated at the CPCM level as described in the Computational Details section (note that the number of species with the same charge is preserved in these processes). The ΔG_s of protolysis of **3** was calculated as ΔG_s(P3) = ΔG_s(P1) + $\Delta G_s(2)$ − $\Delta G_s(1)$ (Table 2).

An inspection of the estimated ΔG_s values of protolysis indicates that (i) the most acidic complexes are those of Ga^{3+} and the least acidic species are those of La^{3+} (water protolysis) and Y^{3+} (H_2O_2 protolysis), (ii) coordinated H_2O_2 is noticeably more acidic than water (by 1.2−10.0 kcal/mol), and (iii) the difference between acidity of ligated H_2O_2 and that of H_2O is the highest for La^{3+} and Al^{3+} and the lowest for Sc^{3+}.

Table 2. Calculated ΔG_s Values (in kcal/mol) of the Processes Involved in the Thermodynamic Cycle in Figure 5 and Experimental pK_a Values of 1

metal	$\Delta G_s(1)$	$\Delta G_s(2)$	pK_a(1)	ΔG_s(P1)	ΔG_s(P3)
Al	10.9[a]	3.7[a]	5.0[b]	9.2[a]	2.0[a]
Ga	9.6	4.3	2.6[b]	5.9	0.6
In	9.5	3.9	4.0[b]	7.8	2.2
Sc	8.7	7.5	4.3[b]	8.2	7.0
Y	7.7	2.2	7.7[b]	12.9	7.3
La	8.5	−1.5	8.5[b]	14.0	4.0

[a]Reference 14. [b]Reference 44.

4. Formation of the Second Hydrogen Peroxide Complex. In the presence of H_2O_2, a similar reaction of substitution of a water ligand for the H_2O_2 molecule may also occur in the hydroperoxo species **5** affording the complexes $[M(H_2O)_4(H_2O_2)(OOH)]^{2+}$ (M = Ga (**6Ga**), In (**6In**), Sc (**6Sc**)), $[Y(H_2O)_6(H_2O_2)(OOH)]^{2+}$ (**6Y**), and $[La(H_2O)_7(H_2O_2)(OOH)]^{2+}$ (**6La**). The same three possible mechanisms (i.e., dissociative, associative, and concerted ones) were examined for this process.

i. Dissociative Mechanism. This mechanism was found for all metals (Scheme 7, D) and it includes the formation of

Scheme 7. Dissociative (D), Associative (A), and Interchange (I_a) Mechanisms of the Water Substitution for H_2O_2 in the Hydroperoxo Complexes 5[a]

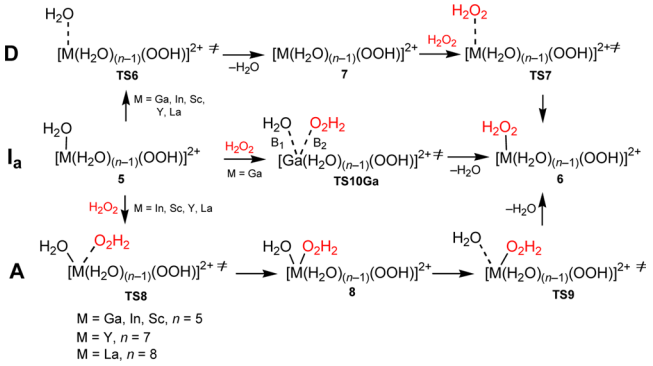

[a]Wiberg bond indices B_1 and B_2 for the breaking and forming bonds are indicated for **TS10Ga**.

intermediates with reduced coordination number of the metal $[M(H_2O)_4(OOH)]^{2+}$ (M = Ga (**7Ga**), In (**7In**), Sc (**7Sc**)), $[Y(H_2O)_6(OOH)]^{2+}$ (**7Y**), and $[La(H_2O)_7(OOH)]^{2+}$ (**7La**) via transition states **TS6**. For the hexa-coordinated species **5Ga**, **5In**, and **5Sc**, two pathways are possible depending on the position of the water molecule eliminated in **5**, that is, the *trans*-pathway and the *cis*-pathway. The latter pathway is slightly more favorable for Ga and In and slightly less favorable for Sc.

In **5Y** and **5La**, there are several nonequivalent water molecules that can be eliminated (Figure 6). Hence, several transition states from **5Y** (**5La**) to **7Y** (**7La**) were found (**TS6a−dY**, **TS6a−cLa**). The pathways via **TS6aY** and **TS6aLa** are the most favorable.

Several possible isomers were also found for the second H_2O_2 adducts **6**. The most kinetically accessible and thermodynamically stable isomers are *cis*-**6Ga**, *cis*-**6In**, and *trans*-**6Sc** (via *cis*-**TS7Ga**, *cis*-**TS7In**, and *trans*-**TS7Sc**). In the case of Y and La, the most stable isomers correspond to square antiprism (**6aY**) or tricapped trigonal prism (**6aLa**) polyhedra with neighboring positions of the H_2O_2 and OOH^- ligands (Figure 6). The first step of the substitution (**5** → **TS6** → **7**) is the rate-limiting one for Ga, In, and Sc whereas the second step (**7** → **TS7** → **6**) is the rate-limiting one for Y and La.

ii. Associative Mechanism. This mechanism was found for all metals except Ga, and it involves the formation of intermediates $[M(H_2O)_5(H_2O_2)(OOH)]^{2+}$ (M = In (**8In**), Sc (**8Sc**)), $[Y(H_2O)_7(H_2O_2)(OOH)]^{2+}$ (**8Y**) and $[La(H_2O)_8$-

dx.doi.org/10.1021/cs400155q | ACS Catal. 2013, 3, 1195−1208

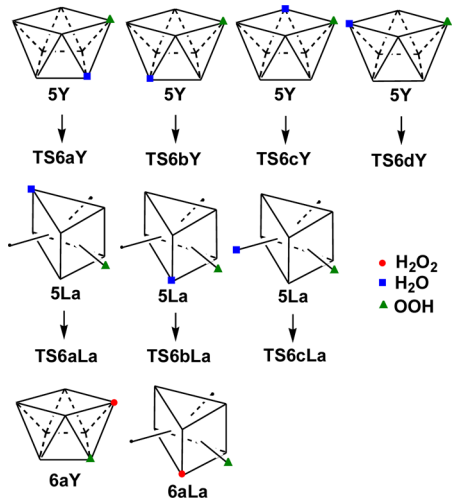

Figure 6. Coordination polyhedra of **5Y**, **5La**, **6aY**, and **6aLa**. In **5Y** and **5La**, the nonequivalent H_2O molecules eliminating upon the formation of **TS6** are shown. Other water ligands and metal atoms are omitted. For other isomers of **6Y** and **6La**, see Tables S3–S5, Supporting Information.

$(H_2O_2)(OOH)]^{2+}$ (**8La**) upon addition of the H_2O_2 molecule to **5** via **TS8** (Scheme 7, A). The intermediate **8** is then converted into the H_2O_2 adduct **6** via **TS9**. A number of possible isomers of intermediates **8** and a number of various transition states **TS9** of the elimination of H_2O molecule from different nonequivalent positions were calculated (see Figures S2 and S3 in Supporting Information), and the most stable ones (**8a** and **TS9a**) are shown in Figure 7. The rate-limiting step of this mechanism is the second one for all metals. In the case of Ga, no intermediate of the associative type was found.

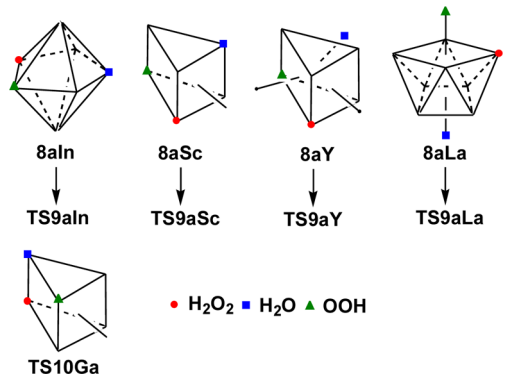

Figure 7. Coordination polyhedra of **8a** and **TS10Ga**. Only the nonequivalent water ligands eliminating upon the formation of **TS9** or **TS10Ga** are shown.

iii. Concerted (Interchange) Mechanism. This mechanism was found only for Ga and involves the formation of transition state **TS10Ga** (Scheme 7, I_a). The structure of **TS10Ga** is a distorted capped trigonal prism with the leaving and entering ligands situated in the neighboring positions (Figure 7). The lengths of the breaking and making bonds in TS are comparable (2.320 and 2.371 Å for the Ga–O_2H_2 and Ga–OH_2 bonds, respectively). For the reaction **5Ga** → **TS10Ga** → **6Ga**, the following parameters were obtained: $\delta B_1 = 0.29$, $\delta B_2 = 0.94$, $S_y = 0.47$, and $\delta B_{av} = 0.61$. These values indicate that the concerted mechanism clearly has associative character (I_a) with the Ga–O_2H_2 bond formation preceding the Ga–OH_2 bond cleavage by 53%, and **TS10Ga** is slightly "late" on the reaction path.

iv. Activation and Reaction Energies. The analysis of the activation and reaction energies (Table 3, Figure 3) indicates

Table 3. Calculated Gibbs Free Energies of Activation ($\Delta G_s^{\ddagger}$) and Reaction (ΔG_s) in Solution (in kcal/mol) for the H_2O-for-H_2O_2 Substitution in 5

metal	mechanism type	reaction	$\Delta G_s^{\ddagger}$	ΔG_s
Al	D	**5Al** → **7Al** (*cis*)	17.4[a]	8.5[a]
		7Al → *cis*-**6Al** (*cis*)	5.6[a]	1.2[a]
Ga	D	**5Ga** → **7Ga** (*cis*) via **TS6Ga**	12.9	5.8
		7Ga → *cis*-**6Ga** (*cis*) via **TS7Ga**	3.8	2.3
	I_a	**5Ga** → *cis*-**6Ga** via **TS10Ga**	22.5	8.1
In	D	**5In** → **7In** (*cis*) via **TS6In**	17.3	12.3
		7In → *cis*-**6In** (*cis*) via **TS7In**	2.8	−3.7
	A	**5In** → **8aIn** via **TS8aIn**	10.4	10.1
		8aIn → *cis*-**6In** via **TS9aIn**	3.9	−1.4
Sc	D	**5Sc** → **7Sc** (*trans*) via **TS6Sc**	16.8	13.4
		7Sc → *trans*-**6Sc** (*trans*) via **TS7Sc**	0.7	−6.0
	A	**5Sc** → **8aSc** via **TS8aSc**	7.5	3.7
		8aSc → *trans*-**6Sc** via **TS9aSc**	6.1	3.7
Y	D	**5Y** → **7aY** via **TS6aY**	6.5	4.7
		7aY → **6aY** via **TS7aY**	3.1	−0.9
	A	**5Y** → **8aY** via **TS8aY**	7.0	4.6
		8aY → **6aY** via **TS9aY**	3.6	−0.9
La	D	**5La** → **7aLa** via **TS6aLa**	8.7	4.0
		7aLa → **6aLa** via **TS7aLa**	5.2	−1.2
	A	**5La** → **8aLa** via **TS8aLa**	5.7	4.8
		8aLa → **6aLa** via **TS9aLa**	3.2	−2.0

[a]Reference 14.

the following: First, the most favorable mechanisms for the second H_2O-for-H_2O_2 substitution are of the dissociative type D for Al,[14] Ga, and Y and of the associative type A for In, Sc, and La. Other mechanisms found for Ga (I_a) and In and Sc (D) are clearly less plausible, while those found for Y (A) and La (D) are only slightly less favorable (by 0.4–1.1 kcal/mol). Second, the overall activation barrier of the formation of the second H_2O_2 adduct **6** relative to **5** decreases along the row of the metals Al > In > Ga > Sc > La > Y keeping the same trend that was found for the generation of the first H_2O_2 adduct **3** except the last two metals. Third, the adduct **6** is noticeably endoergonic relative to the hydroperoxo complex **5** in the case of Al, Ga, In, and Sc (by 8.0–9.7 kcal/mol), while the ΔG_s value of this process for Y and La is smaller (3.8 and 2.8 kcal/mol, respectively).

5. The HO• Radical Generation. In the systems under study, the HO• radicals may be formed upon cleavage of the O–O bond either in the H_2O_2 or the OOH^- ligand (Scheme 8). On the pathways discussed above from the initial aqua complexes **1** to the key complexes **6**, there are several species bearing the coordinated H_2O_2 molecule or the OOH^- ligand that can be a potential source of the HO• radical, that is, **3**–**8**. The calculated adiabatic energies of the homolytic O–O bond cleavage in complexes **3**–**8** and in free H_2O_2 are given in Table 4. The analysis of these energies indicates the following. First, simple coordination of H_2O_2 to the metal in aqua complexes **3** and **4** does not activate hydrogen peroxide since the O–O

dx.doi.org/10.1021/cs400155q | ACS Catal. 2013, 3, 1195–1208

Scheme 8. Formation of the HO• Radical

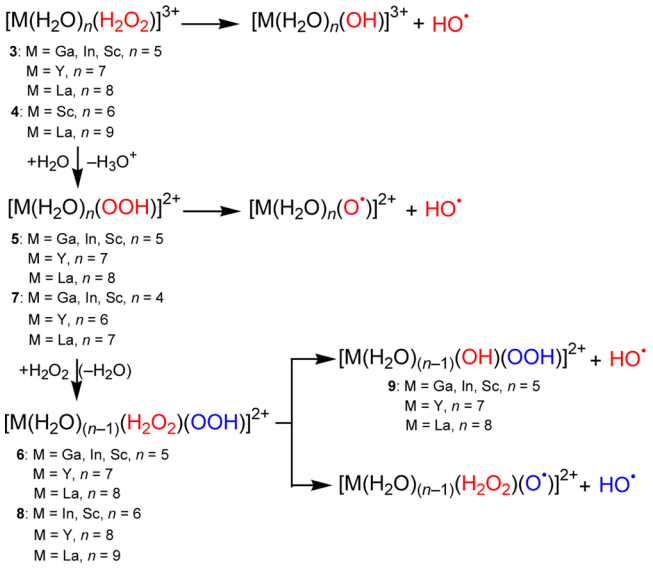

bond energies in these complexes and in free H_2O_2 are similar. Second, the O−O bond energies of the hydroperoxo ligand in complexes **5** and **7** are also similar to that in free H_2O_2. Hence, these species also cannot be a source of the HO• radicals. It is interesting that decomposition of the hydroperoxo ligand is an efficient way of HO• radical generation for catalysts based on *transition metal* complexes $[ML_n(OOH)]^{m+}$. In this case, the decomposition product $[ML_n(-O)^{\bullet}]^{m+}$ is stabilized by an electron transfer from the metal to give $[ML_n(=O)]^{m+}$ (ref 8d) or by delocalization of the electron spin density among coligands and the metal atom.[46] In the case of nontransition metals studied in this work, such a transfer or a delocalization is not possible, which explains the high stability of the OOH^- ligand in **5** and **7** toward the homolytic decomposition.

Third, the joint presence of the OOH^- and H_2O_2 ligands in complexes **6** or **8** tremendously activates the hydrogen peroxide. The HO−OH bond energy in these species is in the range of 4.4−15.3 kcal/mol, which is lower by 24.1−35.0 kcal/mol than that in free H_2O_2 (Table 4). It is interesting that the cleavage of the O−O bond of the OOH^- ligand in **6** requires only slightly lower energy compared with complexes **5**, that is, in contrast to the H_2O_2 ligand, the OOH^- ligand is not activated in **6**.

A role of the OOH^- coligand in the activation of H_2O_2 coordinated in **6** may be understood by analyzing the electronic structure of complexes **9**. For these species, three resonance structures may be drawn (Figure 8), that is, those with the unpaired electron at the O atom of the OH group (**a**) or at an O atom of the OOH ligand (**b** and **c**). In accord with the analyses of the natural bond orbitals and of the spin density distribution (Figure 9), the contribution of the resonance **a** is close to zero. The unpaired electron is delocalized between the O atoms of the OOH ligand with the contributions of resonances **b** and **c** of ca. 2:1. Such a delocalization of the spin density among the OOH ligand stabilizes complexes **9** and, hence, provides the significant activation of the H_2O_2 ligands toward the homolytic O−O bond cleavage.

Another important feature of structures **9** is the oxidation state of the oxygen atoms. All oxygen atoms of both OOH^- and H_2O_2 ligands in **6** have oxidation state −1. Despite the reaction **6** → **9** + HO• being a homolytic process, it results in an intramolecular oxidation−reduction. Indeed, in both resonance structures **b** and **c** of **9**, the oxidation state of the hydroxide oxygen is −2 while the oxidation states of the hydroperoxide oxygen atoms are 0 and −1 (Figure 8). Thus, the homolytic HO−OH bond cleavage in **6** leads to reduction of the OH ligand and to oxidation of the OOH^- ligand. Apparently, the

Table 4. Calculated Adiabatic ΔG_s Values of the Homolytic O−O Bond Dissociation (ΔG_s^{OH}, in kcal/mol) in Free H_2O_2 and Complexes 3−8

reaction	ΔG_s^{OH}
Free H_2O_2	
$H_2O_2 \rightarrow 2HO^{\bullet}$	39.4
Complexes **3**	
$[Ga(H_2O)_5(H_2O_2)]^{3+}$ (**3Ga**) → $[Ga(H_2O)_5(OH)]^{3+}$ + HO•	42.4
$[In(H_2O)_5(H_2O_2)]^{3+}$ (**3In**) → $[In(H_2O)_5(OH)]^{3+}$ + HO•	44.1
$[Sc(H_2O)_5(H_2O_2)]^{3+}$ (**3Sc**) → $[Sc(H_2O)_5(OH)]^{3+}$ + HO•	43.3
$[Y(H_2O)_7(H_2O_2)]^{3+}$ (**3Y**) → $[Y(H_2O)_7(OH)]^{3+}$ + HO•	38.8
$[La(H_2O)_8(H_2O_2)]^{3+}$ (**3La**) → $[La(H_2O)_8(OH)]^{3+}$ + HO•	37.7
Complexes **4**	
$[Sc(H_2O)_6(H_2O_2)]^{3+}$ (**4Sc**) → $[Sc(H_2O)_6(OH^{\bullet})]^{3+}$ + HO•	40.8
$[La(H_2O)_9(H_2O_2)]^{3+}$ (**4La**) → $[La(H_2O)_9(OH^{\bullet})]^{3+}$ + HO•	38.0
Complexes **5**	
$[Ga(H_2O)_5(OOH)]^{2+}$ (**5Ga**) → $[Ga(H_2O)_5(O^{\bullet})]^{2+}$ + HO•	38.4
$[In(H_2O)_5(OOH)]^{2+}$ (**5In**)→ $[In(H_2O)_5(O^{\bullet})]^{2+}$ + HO•	39.7
$[Sc(H_2O)_5(OOH)]^{2+}$ (**5Sc**)→ $[Sc(H_2O)_5(O^{\bullet})]^{2+}$ + HO•	42.5
$[Y(H_2O)_7(OOH)]^{2+}$ (**5Y**)→ $[Y(H_2O)_7(O^{\bullet})]^{2+}$ + HO•	41.6
$[La(H_2O)_8(OOH)]^{2+}$ (**5La**)→ $[La(H_2O)_8(O^{\bullet})]^{2+}$ + HO•	42.3
Complexes **6**	
cis-$[Ga(H_2O)_4(H_2O_2)(OOH)]^{2+}$ (*cis*-**6Ga**) → *cis*-$[Ga(H_2O)_4(OH)(OOH)]^{2+}$ (**9**) + HO•	6.2
cis-$[In(H_2O)_4(H_2O_2)(OOH)]^{2+}$ (*cis*-**6In**) → *cis*-$[In(H_2O)_4(OH)(OOH)]^{2+}$ (**9**) + HO•	7.5
trans-$[Sc(H_2O)_4(H_2O_2)(OOH)]^{2+}$ (*trans*-**6Sc**) → *trans*-$[Sc(H_2O)_4(OH)(OOH)]^{2+}$ (**9**) + HO•	4.4
$[Y(H_2O)_6(H_2O_2)(OOH)]^{2+}$ (**6aY**) → $[Y(H_2O)_6(OH)(OOH)]^{2+}$ (**9**) + HO•	10.3
$[La(H_2O)_7(H_2O_2)(OOH)]^{2+}$ (**6aLa**) → $[La(H_2O)_7(OH)(OOH)]^{2+}$ (**9**) + HO•	15.3
cis-$[Ga(H_2O)_4(H_2O_2)(OOH)]^{2+}$ (*cis*-**6Ga**) → *cis*-$[Ga(H_2O)_4(H_2O_2)(O^{\bullet})]^{2+}$ + HO•	37.2
cis-$[In(H_2O)_4(H_2O_2)(OOH)]^{2+}$ (*cis*-**6In**) → *cis*-$[In(H_2O)_4(H_2O_2)(O^{\bullet})]^{2+}$ + HO•	38.6
trans-$[Sc(H_2O)_4(H_2O_2)(OOH)]^{2+}$ (*trans*-**6Sc**) → *trans*-$[Sc(H_2O)_4(H_2O_2)(O^{\bullet})]^{2+}$ + HO•	40.7
$[Y(H_2O)_6(H_2O_2)(OOH)]^{2+}$ (**6aY**) → $[Y(H_2O)_6(H_2O_2)(O^{\bullet})]^{2+}$ + HO•	42.0
$[La(H_2O)_7(H_2O_2)(OOH)]^{2+}$ (**6aLa**) → $[La(H_2O)_7(H_2O_2)(O^{\bullet})]^{2+}$ + HO•	42.3
Complexes **7**	
$[Ga(H_2O)_4(OOH)]^{2+}$ (**7Ga**) → $[Ga(H_2O)_4(O^{\bullet})]^{2+}$ + HO•	37.9
$[In(H_2O)_4(OOH)]^{2+}$ (**7In**) → $[In(H_2O)_4(O^{\bullet})]^{2+}$ + HO•	38.9
$[Sc(H_2O)_4(OOH)]^{2+}$ (**7Sc**) → $[Sc(H_2O)_4(O^{\bullet})]^{2+}$ + HO•	40.5
$[Y(H_2O)_6(OOH)]^{2+}$ (**7Y**) → $[Y(H_2O)_6(O^{\bullet})]^{2+}$ + HO•	42.1
$[La(H_2O)_7(OOH)]^{2+}$ (**7La**) → $[La(H_2O)_7(O^{\bullet})]^{2+}$ + HO•	41.8
Complexes **8**	
$[In(H_2O)_5(H_2O_2)(OOH)]^{2+}$ (**8aIn**) → $[In(H_2O)_5(OH)(OOH)]^{2+}$ + HO•	5.5
$[Sc(H_2O)_5(H_2O_2)(OOH)]^{2+}$ (**8aSc**) → $[Sc(H_2O)_5(OH)(OOH)]^{2+}$ + HO•	8.2
$[Y(H_2O)_7(H_2O_2)(OOH)]^{2+}$ (**8aY**) → $[Y(H_2O)_7(OH)(OOH)]^{2+}$ + HO•	7.7
$[La(H_2O)_8(H_2O_2)(OOH)]^{2+}$ (**8aLa**) → $[La(H_2O)_8(OH)(OOH)]^{2+}$ + HO•	13.3
Complex *cis*-$[Ga(H_2O)_4(H_2O_2)(OH)]^{2+}$	
cis-$[Ga(H_2O)_4(H_2O_2)(OH)]^{2+} \rightarrow$ *cis*-$[Ga(H_2O)_4(OH)_2]^{2+}$ + HO•	30.8

dx.doi.org/10.1021/cs400155q | ACS Catal. 2013, 3, 1195−1208

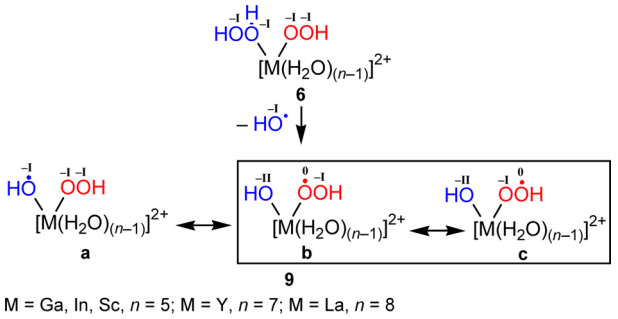

Figure 8. Resonance structures of **9** and oxygen oxidation states in **6** and **9**. The stable resonance structures are boxed.

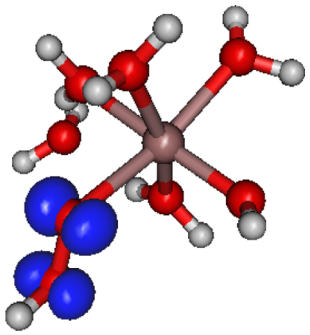

Figure 9. Distribution of spin density in *cis*-**9Ga**.

ability of the OOH^- ligand to be easily oxidized is another driving force of the H_2O_2 activation in **6**. Indeed, the replacement of the OOH^- ligand in *cis*-**6Ga** for another harder oxidizable one (i.e., for the OH^- ligand) dramatically enhances the HO−OH bond energy (Table 4, last entry).

The redox behavior of **6** upon $HO^•$ elimination may also be interpreted in terms of the frontier molecular orbital (MO) composition. Two highest occupied MOs (HOMOs) of **6** are centered at the OOH^- ligand (two orthogonal π^*OO_{OOH} orbitals) whereas the lowest unoccupied MO (LUMO) of **6** is mostly localized at the H_2O_2 ligand ($\sigma^*OO_{H_2O_2}$ orbital) (Figure 10A). When the HO−OH bond is elongated, the electron density starts to shift from the HOMO to the LUMO,

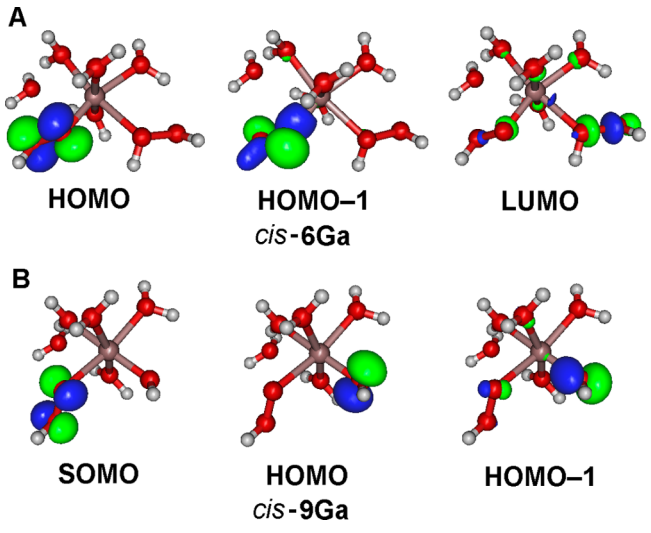

Figure 10. Plots of frontier molecular orbitals of *cis*-**6Ga** and *cis*-**9Ga**.

and this corresponds to the intramolecular oxidation of the OOH^- ligand and the reduction of H_2O_2. After the elimination of $HO^•$, the π^*OO_{OOH} orbital in **9** becomes singly occupied (SOMO), while two doubly occupied HOMOs are centered at the OH^- ligand (Figure 10B). Such changes of the frontier MOs indicate that the redox process involves the OOH^- and H_2O_2 ligands without participation of the metal atom. Thus, the main role of the metal atom in the HO−OH bond cleavage is a simple fixation of both H_2O_2 and OOH^- species in one molecule.

The analysis of electronic structures of **6** and **9** suggests that the OOH^- coligand in the key complex **6** plays the same role as the transition metal does in the classical Fenton or Fenton-like processes, that is, the oxidation of these species (OOH^- or the transition metal) stabilizes the product of the HO−OH bond cleavage and, hence, activates the coordinated H_2O_2 molecule toward the $HO^•$ radical generation.

Additional details of the $HO^•$ radical elimination from **6** including results of the singlet and triplet biradical potential energy surface scans may be found in the Supporting Information.

The H_2O_2 activation toward the homolytic O−O bond cleavage in **6** is the highest for Sc and the lowest for Y and La, the ΔG_s values of the O−O bond dissociation being 4.4, 10.3, and 15.3 kcal/mol, respectively (Table 4). Within each subgroup of the metals IIIA (Al, Ga, In) and IIIB (Sc, Y, La), the H_2O_2 activation decreases along the subgroup. There is a correlation between vertical gas-phase energies of the M−O_2H_2 and HO−OH bonds in **6** (i.e., the energies of decomposition of **6** into corresponding fragments with unrelaxed geometries). Generally, the stronger binding of H_2O_2 to the metal (the stronger M−O_2H_2 bond) corresponds to the higher activation of H_2O_2 (the weaker O−O bond). This correlation is very good for the six-coordinated metals (R^2 = 0.98, Figure 11A), while points associated with Y and La are a bit out of the trend. The higher coordination numbers of Y and La are conceivably responsible for such deviation.

The found trend may be interpreted with help of the NBO analysis, which shows that the occupation of the antibonding σ^*(OO) natural bond orbital increases by 3−28 me upon coordination of H_2O_2 by the metal. Moreover, the vertical HO−OH bond energy demonstrates the clear dependence on the σ^*(OO) NBO occupation (Figure 11B). Thus, the stronger binding of H_2O_2 to a metal provides the higher occupation of the σ^*(OO) NBO and, therefore, the weaker O−O bond.

Summarizing, the joint presence of the H_2O_2 and OOH^- ligands in complexes **6** of the group III elements dramatically activates the hydrogen peroxide molecule toward the homolytic O−O bond cleavage. Such an activation of H_2O_2 is controlled by three main factors: (i) the strength of the H_2O_2 binding to the metal, (ii) the delocalization of the spin density in the product of the O−O bond cleavage, and (iii) the ability of a coligand to be easily oxidized.

Involvement of the third hydrogen peroxide molecule in the mechanism was also considered; however, in this case, the $HO^•$ radical generation requires higher energy (see Supporting Information for discussion).

6. Closure of the Catalytic Cycle. At the final steps of the catalytic cycle, the coordinatively unsaturated complexes $[M(H_2O)_4(OH)]^{2+}$ (M = Ga (**10Ga**), In (**10In**), Sc (**10Sc**)), $[Y(H_2O)_6(OH)]^{2+}$ (**10Y**), and $[La(H_2O)_7(OH)]^{2+}$ (**10La**) are formed as a result of the $HO^•$ and $HOO^•$ elimination from **6** (Scheme 9). Finally, the saturation of the coordination sphere

dx.doi.org/10.1021/cs400155q | ACS Catal. 2013, 3, 1195−1208

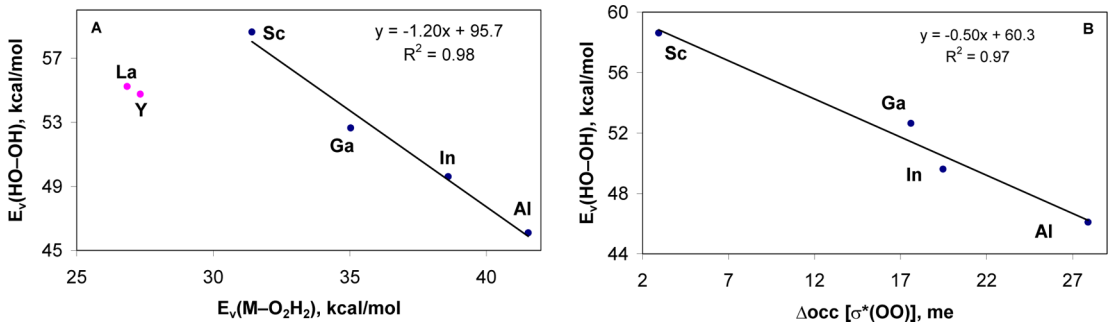

Figure 11. Plot of vertical HO−OH bond energy [E_v(HO−OH)] vs vertical M−O_2H_2 bond energy [E_v(M−O_2H_2)] in **6** (A) and difference of the σ^*(OO) NBO occupations in free H_2O_2 and in **6** (Δocc[σ^*(OO)]) (B).

Scheme 9. Formation of the HO• and HOO• Radicals and Closure of the Catalytic Cycle

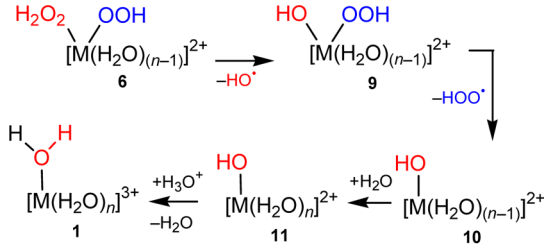

M = Ga, In, Sc, n = 5
M = Y, n = 7
M = La, n = 8

of the metal with water molecule leads to the hydroxo complexes $[M(H_2O)_5(OH)]^{2+}$ (M = Ga (**11Ga**), In (**11In**), Sc **11Sc**), $[Y(H_2O)_7(OH)]^{2+}$ (**11Y**), and $[La(H_2O)_8(OH)]^{2+}$ (**11La**), which can be protonated giving **1** and thus completing the catalytic cycle.

7. Energy Profile. The energy profiles of the reactions are given in Figure 3. The inspection of these profiles indicates that for all the metals Ga, In, Sc, Y, and La, the rate-limiting step of the overall reaction is the monomolecular HO• elimination in complex **6** (**6** → **9**). This situation is different from that found previously for the Al systems[14] for which the second H_2O-for-H_2O_2 substitution appears to be the rate-limiting step.

The HO• radical generation is the endoergonic process. However, the subsequent reaction of HO• with alkane molecule and the following formation of ROOH, alcohol, and ketone (Scheme 1) is highly exoergonic overall. The decrease of the Gibbs free energy of the system at this stage is a driving force of the whole process of the alkane oxidation with H_2O_2 catalyzed by **1**.

In general, the catalytic activity of the aqua complexes of the group III metals depends on three main factors that contribute to the overall activation barrier, that is, (i) the lability of the aqua complexes, (ii) their acidity, and (iii) the H_2O_2 activation toward the homolytic O−O bond cleavage. Complexes of the nontransition metals of the subgroup IIIA (Al, Ga, In) are characterized by a low lability and, hence, comparatively high activation barriers of the H_2O-for-H_2O_2 substitution steps (12.9−17.9 kcal/mol). At the same time, these complexes are highly acidic (i.e., exhibit low energy of deprotonation of the coordinated H_2O_2 molecule), and the H_2O_2 activation is high (the O−O bond energies in **6** are 6.1−7.6 kcal/mol).

Complexes of the heavier transition metals Y and La, in contrast, are highly labile (activation barriers of the substitution steps are 5.3−8.0 kcal/mol) but less acidic and provide lower H_2O_2 activation (the O−O bond energies in **6** are 10.3 and 15.3 kcal/mol). Finally, the Sc species exhibits intermediate properties characterized by the moderate lability, low acidity, but high H_2O_2 activation.

As a result of the combination and partial cancellation of all these factors, the overall activation barriers of the HO• generation[47] for all metals under study do not differ much from each other being in the range of 19.5−25.2 kcal/mol (Table 5). Nevertheless, these values are lower than the activation barrier calculated for Al (25.6 kcal/mol).[14] Thus, other metals of group III are predicted to be even better catalysts for the HO• generation and, hence, for the radical oxidation of alkanes than Al for which experimental data are available.[13] The overall activation barrier increases along the row of the metals Ga < Sc < In ≈ Y < La ≈ Al. Therefore, Ga seems to be the most promising metal for this reaction.

Table 5. Overall Gibbs Free Energies of Activation (in kcal/mol) for the Generation of the HO• Radical in the Systems $[M(H_2O)_n]^{3+}/H_2O_2/CH_3CN-H_2O$

M	$\Delta G^{\ddagger}_{s,ov}$
Al	25.6[a]
Ga	19.5
In	23.5
Sc	22.2
Y	23.7
La	25.2

[a]Reference 14.

FINAL REMARKS

Metals with just one stable nonzero oxidation state (e.g., those of group III) are promising but clearly underexplored catalysts for the oxidation of alkanes with H_2O_2, which occurs via a radical mechanism involving highly reactive HO• radicals. The mechanism of the HO• radical generation catalyzed by complexes of these elements should be of a fundamentally different type than the accepted mechanisms for this process catalyzed by transition metals exhibiting several relatively stable oxidation states. In this work, we extended our previous theoretical study of the HO• radical formation from H_2O_2 catalyzed by the simple aqua complex $[Al(H_2O)_6]^{3+}$ (ref 14) to other metals M of group III (M = Ga, In, Sc, Y, and La).

The general mechanism of the HO• radical generation in the systems $[M(H_2O)_m]^{3+}/H_2O_2$ consists of five principal stages (Scheme 4), that is, (i) substitution of a water ligand for H_2O_2

dx.doi.org/10.1021/cs400155q | ACS Catal. 2013, 3, 1195−1208

molecule, (ii) protolysis of the coordinated H_2O_2, (iii) substitution of the second H_2O for hydrogen peroxide, (iv) generation of the $HO^•$ radical upon homolytic O−O bond cleavage in the H_2O_2 ligand of the key complex $[M(H_2O)_{(m-2)}(H_2O_2)(OOH)]^{2+}$, and (v) closure of the catalytic cycle. The rate-limiting step of the whole process is the monomolecular $HO^•$ elimination from $[M(H_2O)_{(m-2)}(H_2O_2)(OOH)]^{2+}$.

The substitution steps proceed via the limiting dissociative mechanism D for M = Al, Ga, and Y, the limiting associative pathway A for M = Sc and La, and the interchange I_a or the associative A mechanisms for the first or second substitution, respectively, in the case of M = In. The calculated activation barriers of these steps decrease in the order of metals Al > In > Ga > Sc > Y ≥ La, and they are in very good agreement with the experimental data for the related water exchange processes.

There are three main factors determining the catalytic activity of $[M(H_2O)_m]^{3+}$ toward the $HO^•$ radical generation, that is, (i) lability of the complexes, (ii) acidity of the metal-bound ligands, and (iii) H_2O_2 activation toward the homolytic O−O bond cleavage. The presence of the OOH^- coligand in the key species $[M(H_2O)_{(m-2)}(H_2O_2)(OOH)]^{2+}$ is crucial for the tremendous activation of H_2O_2 in these complexes. Such an activation is controlled by three main factors, that is, (i) strength of the H_2O_2 binding to the metal, (ii) delocalization of the spin density among two oxygen atoms of the $OOH^•$ coligand, and (iii) ability of the OOH^- coligand to be easily oxidized.

The calculations predict that the catalytic activity of the aqua complexes $[M(H_2O)_m]^{3+}$ for the hydroxyl radical generation increases along the row of the metals Al ≈ La < Y ≈ In < Sc < Ga. Hence, other metals of group III are even more promising as catalysts for the homogeneous oxidation of alkanes with H_2O_2 than Al for which experimental data are available.

■ ASSOCIATED CONTENT

Supporting Information

Discussion of the nature of **TS3La** and **TS4La**, results of the singlet and triplet biradical potential energy surface scans of the $HO^•$ elimination from **6Al**, tables with calculated absolute and relative energies and Cartesian atomic coordinates for the equilibrium structures. This information is available free of charge via Internet at http://pubs.acs.org.

■ AUTHOR INFORMATION

Corresponding Author

*E-mail: max@mail.ist.utl.pt (M.L.K.).

Notes

The authors declare no competing financial interest.

■ ACKNOWLEDGMENTS

This work was supported by the Fundação para a Ciência e a Tecnologia (FCT), Portugal (Projects PTDC/QUI-QUI/119561/2010 and PTDC/QUI-QUI/102150/2008 and grant SFRH/BPD/88473/2012), and the Russian Foundation for Basic Research (grant No. 12-03-00084-a).

■ REFERENCES

(1) (a) Shilov, A. E.; Shul'pin, G. B. *Chem. Rev.* **1997**, *97*, 2879. (b) Shul'pin, G. B. *Mini-Rev. Org. Chem.* **2009**, *6*, 95. (c) Crabtree, R. H. *Chem. Rev.* **1995**, *95*, 987. (d) Jia, C.; Kitamura, T.; Fujiwara, Y. *Acc. Chem. Res.* **2001**, *34*, 633. (e) Lane, B. S.; Burgess, K. *Chem. Rev.* **2003**, *103*, 2457. (f) Grigoropoulou, G.; Clark, J. H.; Elings, J. A. *Green Chem.* **2003**, *5*, 1. (g) Brégeault, J.-M. *Dalton Trans.* **2003**, 3289. (h) Labinger, J. A. *J. Mol. Catal. A* **2004**, *220*, 27. (i) Conley, B. L.; Tenn, W. J., III; Young, K. J. H.; Ganesh, S. K.; Meier, S. K.; Ziatdinov, V. R.; Mironov, O.; Oxgaard, J.; Gonzales, J.; Goddard, W. A., III; Periana, R. A. *J. Mol. Catal. A* **2006**, *251*, 8. (j) Muzart, J. *J. Mol. Catal. A* **2007**, *276*, 62. (k) Díaz-Requejo, M. M.; Pérez, P. J. *Chem. Rev.* **2008**, *108*, 3379. (l) Crabtree, R. H. *Chem. Rev.* **2010**, *110*, 575. (m) da Silva, J. A. L.; Fraústo da Silva, J. J. R.; Pombeiro, A. J. L. *Coord. Chem. Rev.* **2011**, *255*, 2232.

(2) (a) Lam, W. W. Y.; Yiu, S.-M.; Lee, J. M. N.; Yau, S. K. Y.; Kwong, H.-K.; Lau, T.-C.; Liu, D.; Lin, Z. *J. Am. Chem. Soc.* **2006**, *128*, 2851. (b) Bales, B. C.; Brown, P.; Dehestani, A.; Mayer, J. M. *J. Am. Chem. Soc.* **2005**, *127*, 2832. (c) Mayer, J. M. *Acc. Chem. Res.* **1998**, *31*, 441. (d) Spitzer, U. A.; Lee, D. G. *J. Org. Chem.* **1975**, *40*, 2539. (e) Tenaglia, A.; Terranova, E.; Waegell, B. *Tetrahedron Lett.* **1989**, *30*, 5271. (f) Tenaglia, A.; Terranova, E.; Waegell, B. *J. Chem. Soc., Chem. Commun.* **1990**, 1344. (g) Bakke, J. M.; Frøhaug, A. E. *J. Phys. Org. Chem.* **1996**, *9*, 507.

(3) Bray, W. C.; Gorin, M. H. *J. Am. Chem. Soc.* **1932**, *54*, 2124.

(4) Shul'pin, G. B.; Kozlov, Y. N.; Nizova, G. V.; Süss-Fink, G.; Stanislas, S.; Kitaygorodskiy, A.; Kulikova, V. S. *J. Chem. Soc., Perkin Trans. 2* **2001**, 1351.

(5) Haber, F.; Weiss, J. *Naturwissemschaften* **1932**, *20*, 948.

(6) Kozlov, Y. N.; Nadezhdin, A. D.; Purmal', A. P. *Kinet. Katal.* **1973**, *14*, 141.

(7) (a) Sawyer, D. T.; Sobkowiak, A.; Matsushita, T. *Acc. Chem. Res.* **1996**, *29*, 409. (b) Walling, C. *Acc. Chem. Res.* **1998**, *31*, 155. (c) Goldstein, S.; Meyerstein, D. *Acc. Chem. Res.* **1999**, *32*, 547. (d) MacFaul, P. A.; Wayner, D. D. M.; Ingold, K. U. *Acc. Chem. Res.* **1998**, *31*, 159. (e) Dunford, H. B. *Coord. Chem. Rev.* **2002**, *233*, 311. (f) Groves, J. T. *J. Inorg. Biochem.* **2006**, *100*, 434. (g) Bach, R. D.; Dmitrenko, O. *J. Org. Chem.* **2010**, *75*, 3705. (h) Paczesniak, T.; Sobkowiak, A. *J. Mol. Catal. A* **2003**, *194*, 1. (i) Ensing, B.; Buda, F.; Gribnau, M. C. M.; Baerends, E. *J. Am. Chem. Soc.* **2004**, *126*, 4355. (j) Bautz, J.; Bukowski, M. R.; Kerscher, M.; Stubna, A.; Comba, P.; Lienke, A.; Münck, E.; Que, L., Jr. *Angew. Chem., Int. Ed.* **2006**, *45*, 5681. (k) Rachmilovich-Calis, S.; Masarwa, A.; Meyerstein, N.; Meyerstein, D.; van Eldik, R. *Chem.—Eur. J.* **2009**, *15*, 8303. (l) Rush, J. D.; Koppenol, W. H. *J. Inorg. Biochem.* **1987**, *29*, 199. (m) Kremer, M. L. *J. Inorg. Biochem.* **2000**, *78*, 255. (n) Kremer, M. L. J. *J. Phys. Chem. A* **2003**, *107*, 1734. (o) Perez-Benito, J. F. *J. Phys. Chem. A* **2004**, *108*, 4853. (p) Bassan, A.; Blomberg, M. R. A.; Siegbahn, P. E. M.; Que, L. *J. Am. Chem. Soc.* **2002**, *124*, 11056. (q) Comba, P.; Rajaraman, G.; Rohwer, H. *Inorg. Chem.* **2007**, *46*, 3826. (r) Chandrasena, R. E. P.; Vatsis, K. P.; Coon, M. J.; Hollenberg, P. F.; Newcomb, M. *J. Am. Chem. Soc.* **2004**, *126*, 115. (s) Michel, C.; Baerends, E. J. *Inorg. Chem.* **2009**, *48*, 3628. (t) Das, S.; Bhattacharyya, J.; Mukhopadhyay, S. *Dalton Trans.* **2008**, 6634. (u) Nam, W.; Han, H. J.; Oh, S. Y.; Lee, Y. J.; Choi, M. H.; Han, S. Y.; Kim, C.; Woo, S. K.; Shin, W. *J. Am. Chem. Soc.* **2000**, *122*, 8677. (v) Derat, E.; Kumar, D.; Hirao, H.; Shaik, S. *J. Am. Chem. Soc.* **2006**, *128*, 473. (w) Kamachi, T.; Yoshizawa, K. *J. Am. Chem. Soc.* **2003**, *125*, 4652. (x) Ogliaro, F.; Harris, N.; Cohen, S.; Filatov, M.; de Visser, S. P.; Shaik, S. *J. Am. Chem. Soc.* **2000**, *122*, 8977.

(8) (a) Khaliullin, R. Z.; Bell, A. T.; Head-Gordon, M. *J. Phys. Chem. B* **2005**, *109*, 17984. (b) Kirillova, M. V.; Kuznetsov, M. L.; Romakh, V. B.; Shul'pin, L. S.; Fraústo da Silva, J. J. R.; Pombeiro, A. J. L.; Shul'pin, G. B. *J. Catal.* **2009**, *267*, 140. (c) Kirillova, M. V.; Kuznetsov, M. L.; Kozlov, Y. N.; Shul'pin, L. S.; Kitaygorodskiy, A.; Pombeiro, A. J. L.; Shul'pin, G. B. *ACS Catal.* **2011**, *1*, 1511. (d) Kuznetsov, M. L.; Pombeiro, A. J. L. *Inorg. Chem.* **2009**, *48*, 307.

(9) (a) Thomas, J. M.; Raja, R.; Sankar, G.; Bell, R. G. *Acc. Chem. Res.* **2001**, *34*, 191. (b) Schuchardt, U.; Cardoso, D.; Sercheli, R.; Pereira, R.; da Cruz, R. S.; Guerreiro, M. C.; Mandelli, D.; Spinacé, E. V.; Pires, E. L. *Appl. Catal., A* **2001**, *211*, 1. (c) Tchenar, Y. N.; Choukchou-Braham, A.; Bachir, R. *Bull. Mater. Sci.* **2012**, *35*, 673. (d) Ciuffi, K. J.; de Faria, E. H.; Marçal, L.; Rocha, L. A.; Calefi, P. S.; Nassar, E. J.; Pepe, I.; da Rocha, Z. N.; Vicente, M. A.; Trujillano, R.; Gil, A.; Korili, S. A. *ACS Appl. Mater. Interfaces* **2012**, *4*, 2525. (e) Ebadi, A.; Nikbakht, F. *React. Kinet., Mech. Catal.* **2011**, *104*, 37. (f) Kalam, A.;

Rahman, L.; Kumashiro, M.; Ishihara, T. *Catal. Commun.* **2011**, *12*, 1198. (g) Ricci, G. P.; Rocha, Z. N.; Nakagaki, S.; Castro, K. A. D. F.; Crotti, A. E. M.; Calefi, P. S.; Nassar, E. J.; Ciuffi, K. J. *Appl. Catal., A* **2010**, *389*, 147. (h) Borah, P.; Datta, A. *Appl. Catal., A* **2010**, *376*, 19. (i) Sadjadi, M. S.; Ebadi, A.; Zare, K. *React. Kinet., Mech. Catal.* **2010**, *99*, 119. (j) Aboelfetoh, E. F.; Pietschnig, R. *Catal. Lett.* **2009**, *127*, 83. (k) Mac Leod, T. C. O.; Guedes, D. F. C.; Lelo, M. R.; Rocha, R. A.; Caetano, B. L.; Ciuffi, K. J.; Assis, M. D. *J. Mol. Catal. A* **2006**, *259*, 319. (l) Caetano, B. L.; Rocha, L. A.; Molina, E.; Rocha, Z. N.; Ricci, G.; Calefi, P. S.; de Lima, O. J.; Mello, C.; Nassar, E. J.; Ciuffi, K. J. *Appl. Catal., A* **2006**, *311*, 122. (m) Modén, B.; Zhan, B.-Z.; Dakka, J.; Santiesteban, J. G.; Iglesia, E. *J. Catal.* **2006**, *239*, 390. (n) Selvam, P.; Mohapatra, S. K. *J. Catal.* **2006**, *238*, 88. (o) Selvam, P.; Mohapatra, S. K. *J. Catal.* **2005**, *233*, 276. (p) Dapurkar, S. E.; Sakthivel, A.; Selvam, P. *J. Mol. Catal. A* **2004**, *223*, 241. (q) Abbasov, A. A.; Zul'fugarova, S. Z.; Gasanova, L. M.; Nagiev, T. M. *Russ. J. Phys. Chem.* **2002**, *76*, 1591. (r) Avdeev, M. V.; Bagrii, E. I.; Maravin, G. B.; Korolev, Y. M.; Borisov, R. S. *Petrol. Chem.* **2000**, *40*, 391. (s) Zahedi-Niaki, M. H.; Kapoor, M. P.; Kaliaguine, S. *J. Catal.* **1998**, *177*, 231. (t) Luna, F. J.; Ukawa, S. E.; Wallau, M.; Schuchardt, U. *J. Mol. Catal. A* **1997**, *117*, 405. (u) Camblor, M. A.; Corma, A.; Perezpariente, J. *Zeolites* **1993**, *13*, 82.

(10) Aboelfetoh, E. F.; Fechtelkord, M.; Pietschnig, R. *J. Mol. Catal. A* **2010**, *318*, 51.

(11) Mandelli, D.; do Amaral, A. C. N.; Kozlov, Y. N.; Shul'pina, L. S.; Bonon, A. J.; Carvalho, W. A.; Shul'pin, G. B. *Catal. Lett.* **2009**, *132*, 235.

(12) (a) Asadullah, M.; Kitamura, T.; Fujiwara, Y. *Angew. Chem., Int. Ed.* **2000**, *39*, 2475. (b) Asadullah, M.; Kitamura, T.; Fujiwara, Y. *Appl. Organomet. Chem.* **1999**, *13*, 539. (c) Asadullah, M.; Kitamura, T.; Fujiwara, Y. *Catal. Lett.* **2000**, *69*, 37. (d) Asadullah, M.; Kitamura, T.; Fujiwara, Y. *J. Catal.* **2000**, *195*, 180. (e) Asadullah, M.; Taniguchi, Y.; Kitamura, T.; Fujiwara, Y. *Sekiyu Gakkaishi (J. Jpn. Petrol. Inst.)* **1998**, *41*, 236. (f) Asadullah, M.; Taniguchi, Y.; Kitamura, T.; Fujiwara, Y. *Appl. Organomet. Chem.* **1998**, *12*, 277.

(13) Mandelli, D.; Chiacchio, K. C.; Kozlov, Y. N.; Shul'pin, G. B. *Tetrahedron Lett.* **2008**, *49*, 6693.

(14) Kuznetsov, M. L.; Kozlov, Y. N.; Mandelli, D.; Pombeiro, A. J. L.; Shul'pin, G. B. *Inorg. Chem.* **2011**, *50*, 3996.

(15) (a) Becke, A. D. *J. Chem. Phys.* **1993**, *98*, 5648. (b) Lee, C.; Yang, W.; Parr, R. G. *Phys. Rev.* **1988**, *B37*, 785.

(16) Frisch, M. J.; Trucks, G. W.; Schlegel, H. B.; Scuseria, G. E.; Robb, M. A.; Cheeseman, J. R.; Montgomery, J. A., Jr.; Vreven, T.; Kudin, K. N.; Burant, J. C.; Millam, J. M.; Iyengar, S. S.; Tomasi, J.; Barone, V.; Mennucci, B.; Cossi, M.; Scalmani, G.; Rega, N.; Petersson, G. A.; Nakatsuji, H.; Hada, M.; Ehara, M.; Toyota, K.; Fukuda, R.; Hasegawa, J.; Ishida, M.; Nakajima, T.; Honda, Y.; Kitao, O.; Nakai, H.; Klene, M.; Li, X.; Knox, J. E.; Hratchian, H. P.; Cross, J. B.; Bakken, V.; Adamo, C.; Jaramillo, J.; Gomperts, R.; Stratmann, R. E.; Yazyev, O.; Austin, A. J.; Cammi, R.; Pomelli, C.; Ochterski, J. W.; Ayala, P. Y.; Morokuma, K.; Voth, G. A.; Salvador, P.; Dannenberg, J. J.; Zakrzewski, V. G.; Dapprich, S.; Daniels, A. D.; Strain, M. C.; Farkas, O.; Malick, D. K.; Rabuck, A. D.; Raghavachari, K.; Foresman, J. B.; Ortiz, J. V.; Cui, Q.; Baboul, A. G.; Clifford, S.; Cioslowski, J.; Stefanov, B. B.; Liu, G.; Liashenko, A.; Piskorz, P.; Komaromi, I.; Martin, R. L.; Fox, D. J.; Keith, T.; Al-Laham, M. A.; Peng, C. Y.; Nanayakkara, A.; Challacombe, M.; Gill, P. M. W.; Johnson, B.; Chen, W.; Wong, M. W.; Gonzalez, C.; Pople, J. A. *Gaussian 03*, revision B.05; Gaussian, Inc.: Wallingford, CT, 2003.

(17) (a) McLean, A. D.; Chandler, G. S. *J. Chem. Phys.* **1980**, *72*, 5639. (b) Krishnan, R.; Binkley, J. S.; Seeger, R.; Pople, J. A. *J. Chem. Phys.* **1980**, *72*, 650. (c) Wachters, A. J. H. *J. Chem. Phys.* **1970**, *52*, 1033. (d) Hay, P. J. *J. Chem. Phys.* **1977**, *66*, 4377.

(18) (a) Bergner, A.; Dolg, M.; Kuechle, W.; Stoll, H.; Preuss, H. *Mol. Phys.* **1993**, *80*, 1431. (b) Dolg, M.; Stoll, H.; Savin, A.; Preuss, H. *Theor. Chim. Acta* **1989**, *75*, 173.

(19) Andrae, D.; Haeussermann, U.; Dolg, M.; Stoll, H.; Preuss, H. *Theor. Chim. Acta* **1990**, *77*, 123.

(20) Pyykkö, P.; Straka, M.; Tamm, T. *Phys. Chem. Chem. Phys.* **1999**, *1*, 3441.

(21) (a) Guillaume, S. M.; Brignou, P.; Susperregui, N.; Maron, L.; Kuzdrowska, M.; Kratsch, J.; Roesk, P. W. *Polym. Chem.* **2012**, *3*, 429. (b) Rosal, I. D.; Poteaua, R.; Maron, L. *Dalton Trans.* **2011**, *40*, 11228.

(22) Luo, X.; Fleming, P. R.; Rizzo, T. R. *J. Chem. Phys.* **1992**, *96*, 5659.

(23) Gonzalez, C.; Schlegel, H. B. *J. Chem. Phys.* **1991**, *95*, 5853.

(24) Barone, V.; Cossi, M. *J. Phys. Chem.* **1998**, *102*, 1995.

(25) Wertz, D. H. *J. Am. Chem. Soc.* **1980**, *102*, 5316.

(26) Cooper, J.; Ziegler, T. *Inorg. Chem.* **2002**, *41*, 6614.

(27) Wiberg, K. B. *Tetrahedron* **1968**, *24*, 1083.

(28) Reed, A. E.; Curtiss, L. A.; Weinhold, F. *Chem. Rev.* **1988**, *88*, 899.

(29) (a) Moyano, A.; Pericàs, M. A.; Valentí, E. *J. Org. Chem.* **1989**, *54*, 573. (b) Lecea, B.; Arrieta, A.; Roa, G.; Ugalde, G. M.; Cossío, F. P. *J. Am. Chem. Soc.* **1994**, *116*, 9613. (c) Morao, I.; Lecea, B.; Cossío, F. P. *J. Org. Chem.* **1997**, *62*, 7033. (d) Cossío, F. P.; Morao, I.; Jiao, H.; Schleyer, P. v. R. *J. Am. Chem. Soc.* **1999**, *121*, 6737.

(30) (a) Swift, T. J.; Fritz, O. G.; Stephenson, F. A. *J. Chem. Phys.* **1967**, *46*, 406. (b) Fiat, D.; Connick, R. E. *J. Am. Chem. Soc.* **1966**, *88*, 4754. (c) Fratiello, A.; Lee, R. E.; Schuster, R. E. *Inorg. Chem.* **1970**, *9*, 82. (d) Maeda, M.; Ohtaki, H. *Bull. Chem. Soc. Jpn.* **1977**, *50*, 1893.

(31) Rudolph, W. W.; Pye, C. C. *J. Phys. Chem. A* **2000**, *104*, 1627.

(32) (a) Smirnov, P.; Wakita, H.; Yamaguchi, T. *J. Phys. Chem. B* **1998**, *102*, 4802. (b) Lindqvist-Reis, P.; Persson, I.; Sandström, M. *Dalton Trans.* **2006**, 3868.

(33) (a) Díaz-Moreno, S.; Muñoz-Páez, A.; Chaboy, J. *J. Phys. Chem. A* **2000**, *104*, 1278. (b) Habenschuss, A.; Spedding, F. H. *J. Chem. Phys.* **1979**, *70*, 3758. (c) Bukowska-Strzyzewska, M.; Tosik, A. *Acta Crystallogr.* **1982**, *B38*, 950. (d) Rogers, R. D.; Kurihara, L. K. *Inorg. Chim. Acta* **1986**, *116*, 171. (e) Chatterjee, A.; Maslen, E. N.; Watson, K. J. *Acta Crystallogr.* **1988**, *B44*, 381.

(34) Lindqvist-Reis, P.; Muñoz-Páez, A.; Díaz-Moreno, S.; Pattanaik, S.; Persson, I.; Sandström, M. *Inorg. Chem.* **1998**, *37*, 6675.

(35) (a) Helm, L.; Nicolle, G. M.; Merbach, A. E. *Adv. Inorg. Chem.* **2005**, *57*, 327. (b) Richens, D. T. *Chem. Rev.* **2005**, *105*, 1961. (c) Hugi-Cleary, D.; Helm, L.; Merbach, A. E. *J. Am. Chem. Soc.* **1987**, *109*, 4444. (d) Glass, G. E.; Schwabacher, W. B.; Tobias, R. S. *Inorg. Chem.* **1968**, *7*, 2471. (e) Kowall, T.; Foglia, F.; Helm, L.; Merbach, A. E. *Chem.—Eur. J.* **1996**, *2*, 285. (f) Erras-Hanauer, H.; Clark, T.; van Eldik, R. *Coord. Chem. Rev.* **2003**, *238*−*239*, 233.

(36) Langford, C. H.; Gray, H. B. *Ligand Substitution Dynamics*; Benjamin: New York, 1965.

(37) Kuznetsov, M. L.; Kukushkin, V. Yu.; Pombeiro, A. J. L. *Dalton Trans.* **2008**, 1312.

(38) Lincoln, S. F.; Merbach, A. E. *Adv. Inorg. Chem.* **1995**, *42*, 1.

(39) Kowall, T.; Caravan, P.; Bourgeois, H.; Helm, L.; Rotzinger, F. P.; Merbach, A. E. *J. Am. Chem. Soc.* **1998**, *120*, 6569.

(40) (a) Caravan, P.; Toth, E.; Rockenbauer, A.; Merbach, A. E. *J. Am. Chem. Soc.* **1999**, *121*, 10403. (b) Moreau, G.; Helm, L.; Purans, J.; Merbach, A. E. *J. Phys. Chem. A* **2002**, *106*, 3034. (c) Micskei, K.; Powell, D. H.; Helm, L.; Brucher, E.; Merbach, A. E. *Magn. Reson. Chem.* **1993**, *31*, 1011. (d) Cossy, C.; Helm, L.; Merbach, A. E. *Inorg. Chem.* **1988**, *27*, 1973. (e) Cossy, C.; Helm, L.; Merbach, A. E. *Inorg. Chem.* **1989**, *28*, 2699. (f) Caravan, P.; Merbach, A. E. *J. Chem. Soc., Chem. Commun.* **1997**, 2147.

(41) Fay, D. P.; Litchinsky, D.; Purdie, N. *J. Phys. Chem.* **1969**, *73*, 544.

(42) (a) Rotzinger, F. P. *J. Am. Chem. Soc.* **1997**, *119*, 5230. (b) Rotzinger, F. P. *J. Phys. Chem. B* **2005**, *109*, 1510.

(43) Sposito, G. *The Environmental Chemistry of Aluminium*, 2nd ed.; CRC Press: Boca Raton, FL, 1995.

(44) Wulfsberg, G. *Principles of Descriptive Inorganic Chemistry*; University Science Books: Mill Valley, CA, 1991.

(45) Kandioller, W.; Hartinger, C. G.; Nazarov, A. A.; Bartel, C.; Skocic, M.; Jakupec, M. A.; Arion, V. B.; Keppler, B. K. *Chem.—Eur. J.* **2009**, *15*, 12283.

(46) (a) DiPasquale, A. G.; Hrovat, D. A.; Mayer, J. M. *Organometallics* **2006**, *25*, 915. (b) DiPasquale, A. G.; Kaminsky, W.; Mayer, J. M. *J. Am. Chem. Soc.* **2002**, *124*, 14534.

(47) The overall activation barriers of the HO$^{\bullet}$ generation, $\Delta G^{\ddagger}_{s,ov}$, are calculated as $\Delta G^{\ddagger}_{s,ov} = \Delta G_s(S1) + \Delta G_s(P) + \Delta G_s(S2) + \Delta G_s^{OH}$ (except Al), where $\Delta G_s(S1)$, $\Delta G_s(S2)$, $\Delta G_s(P)$, and ΔG_s^{OH} correspond to the first and second substitution steps, protolysis of **3**, and HO$^{\bullet}$ elimination in **6**, respectively.

dx.doi.org/10.1021/cs400155q | *ACS Catal.* 2013, 3, 1195−1208